

LEACHING BEHAVIOR OF ZnO NANOPARTICLES IN MUNICIPAL SOLID
WASTE

by

Emine Tuğçe Sakallıoğlu

B.Sc. in Environmental Engineering, İstanbul University, 2012

Submitted to the Institute of Environmental Sciences
in partial fulfillment of the requirements for the degree of
Master of Science
in
Environmental Technology

Boğaziçi University

2018

ACKNOWLEDGEMENTS

First of all, I would like to express my deepest gratitude to my thesis supervisor Prof. Dr. Burak Demirel for his continuous guidance, kind support and encouragement during this study and also my master education. It was an honor and privilege to work with him.

I am very grateful to Prof. Dr. Nadim K. Coptu, Prof. Dr. Turgut Tüzün Onay, Dr. Ceyda S. Uyguner Demirel and Prof. Dr. Tanju Karanfil their opinion, guidance, friendly approach throughout this study and beyond.

I am also grateful to the Scientific and Technological Research Council of Turkey (TUBITAK) by project number 112Y322.

I would like to express my sincere gratitude to the jury members; Prof. Dr. Ayşen Erdinçler and Prof. Dr. Hüseyin Selçuk for their time and valuable suggestions.

In addition, I would like to thank to and Filiz Ayılmaz, Koray Sakarya and Derya Aydın Sarıkurt for their scientific help and support during the study.

I am also grateful to my friends from the Institute of Environmental Sciences, Zeynep Demiray, Merve Şahan and Başak Kılıç for their unique friendship, encouragement and support during this study and also my master education. I am also grateful my friends Mehmet Ali Hakan, Aslıhan Yolcu, Gizem Tıǧlı, Leyla Durmuş and Burcu Sarıcı.

Finally, I would like to express a deep sense of gratitude to my parents, Emine Sakallıođlu and Arif Sakallıođlu and my brother Burak Sakallıođlu for their constant love, endless encouragement and blessings.

ABSTRACT

LEACHING BEHAVIOR OF ZnO NANOPARTICLES IN MUNICIPAL SOLID WASTE

The use of engineered nanomaterials (ENMs) in commercial products has been increasing in our daily lives and in the industry day by day. Among the ENMs, zinc oxide nanoparticles (ZnO NPs) have been used in many consumer products such as cosmetics, textile, electronics, medicine, paints, agriculture and environmental remediation. As a result of extensive use, ENMs containing wastes end up their life cycle in treatment facilities such as wastewater treatment plants, incineration units and sanitary landfills ultimately. However, there is still a lack of knowledge about the fate and behavior of ENMs in the landfill and landfill leachate. Therefore, in this research it is aimed to investigate the leaching behavior of three different kinds of ZnO NPs such as powder (uncoated), powder Z-Cote HP1 (coated) and dispersion (slurry) in fresh municipal solid waste (MSW). Batch reactors (1 L) were used to observe the leaching potential of ZnO NPs under acidic, basic and high ionic strength (IS) conditions. The reactors were filled with 250 g fresh MSW. Each reactor was loaded 10, 25 and 100 mg/L ZnO NPs. The reactors loaded with ZnO NPs and control reactors were shaken for 72 hours. 10 mL of leachate samples were regularly taken from batch reactors at pre-determined time intervals and they were analyzed for Zn concentration, pH, conductivity and particle size distribution. The results showed that nano-ZnO mass retained in the solid waste matrix with ratio between 84-93%. There was no significant influence of pH and IS on the leaching potential of nano-ZnO.

ÖZET

ZnO NANOPARTİKÜLLERİNİN EVSEL KATI ATIKTAKİ SIZMA DAVRANIŞI

Günlük hayatımızda ve endüstride mühendislik çalışmaları sonucu elde edilmiş (işlenmiş) nanopartiküllerin ticari ürünlerde kullanımı günden güne artmaktadır. İşlenmiş nanopartiküller arasında çinko oksit nanopartikülü (ZnO NP), kozmetik, tekstil, elektronik, ilaç, boya, tarım ve çevre iyileştirme gibi pek çok tüketici ürünlerinde kullanılmaktadır. Yaygın kullanımı sonucunda, işlenmiş nanopartikül içeren ürünler ömrü dolduktan sonra, atık su arıtma tesisleri, yakma üniteleri ve düzenli depolama sahaları gibi nihai bertaraf tesislerine gidecektir. Bununla birlikte, işlenmiş nanopartiküllerin düzenli depolama sahası ve sızıntı suyundaki davranışları ve etkileşimleri hakkında yeterli bilgi mevcut değildir. Bu nedenle, bu çalışmada yüzey kaplamasız, kaplamalı ve dispersiyon formundaki ZnO NP'lerinin, evsel katı atıktaki sızma davranışını incelemek amaçlanmıştır. 1 L'lik cam şişe reaktörler, ZnO NP'lerinin asidik, bazik ve yüksek iyon gücü koşullarındaki sızma potansiyellerini gözlemlemek için kullanılmıştır. Reaktörlere 250 g taze evsel katı atık konulmuştur. Her bir reaktöre 10, 25 ve 100 mg/L ZnO NP eklenmiştir. ZnO NP yüklü reaktörler ve kontrol reaktörleri 72 saat boyunca çalkalanmıştır. Önceden belirlenmiş zaman aralıklarında, 10 mL sızıntı suyu örnekleri düzenli olarak reaktörlerden alınmıştır ve Zn konsantrasyonları, pH, iletkenlik ve partikül boyut dağılımı analiz edilmiştir. Sonuçlara göre, nano ZnO %84-93 oranları arasında katı atıkta kalmıştır. pH, iletkenlik ve yüksek iyon gücünün ZnO sızma potansiyeline belirgin bir etkisinin olmadığı görülmüştür.

5.1. Initial Solid Waste Analysis.....	29
5.2. Leaching Experiments with ZnO NP.....	30
5.2.1. Leaching Experiments with Uncoated ZnO NPs.....	31
5.2.2. Leaching Experiments with Z-Cote HP1 ZnO NPs.....	36
5.2.3. Leaching Experiments with Dispersion ZnO NPs.....	41
5.3. Comparison of Acidic, Basic and High Ionic Strength Reactors for Each Set.....	46
5.4. Particle Size Distribution Analysis.....	54
6. CONCLUSIONS.....	56
7. RECOMMENDATIONS.....	58
REFERENCES.....	59
APPENDIX: THE COMPLETE RESULTS FROM SET 1 TO SET 9.....	66

LIST OF FIGURES

Figure 1.1. Relationship of ENPs growth over time (Amara's law correlation of nanotechnological growth).....	1
Figure 2.1. The classification of nanoparticles.....	4
Figure 2.2. The release of ENMs during their life cycle.....	7
Figure 2.3. Global flow of ENMs in 2010.....	7
Figure 2.4. Global material flows for ZnO ENMs (metric tons/year) in 2010.....	8
Figure 4.1. Components of İzmit İZAYDAŞ MSW.....	19
Figure 4.2. The average particle size of uncoated nano ZnO.....	21
Figure 4.3. The average particle size of Z-Cote HP1 (coated).....	21
Figure 4.4. The ESEM image of Z-Cote HP1 (coated) nano-ZnO.....	22
Figure 4.5. Batch reactors in shaker.....	23
Figure 5.1. The pH change in uncoated ZnO NP-acidic set reactors with time (Set 1).....	32
Figure 5.2. The Zn concentration change in uncoated ZnO NP-acidic set reactors with time (Set 1).....	32
Figure 5.3. The pH change in uncoated ZnO NP-basic set reactors with time (Set 2).....	33
Figure 5.4. The Zn concentration change in uncoated ZnO NP-basic set reactors with time (Set 2).....	33
Figure 5.5. The pH change in uncoated ZnO NP-high IS set reactors with time (Set 3).....	34

Figure 5.6. The conductivity change in uncoated ZnO NP-high IS set reactors with time (Set 3).....	35
Figure 5.7. The Zn concentration change in uncoated-high IS set reactors with time (Set 3).....	35
Figure 5.8. The pH change in Z-Cote HP1 ZnO NP-acidic set reactors with time (Set 4).....	37
Figure 5.9. The Zn concentration change in Z-Cote HP1 ZnO NP-acidic set reactors with time (Set 4).....	37
Figure 5.10. The pH change in Z-Cote HP1-basic set reactors with time (Set 5).....	38
Figure 5.11. The Zn concentration change in Z-Cote HP1-basic set reactors with time (Set 5).....	39
Figure 5.12. The pH change in Z-Cote HP1-high IS set reactors with time (Set 6).....	39
Figure 5.13. The Zn concentration change in Z-Cote HP1-high IS set reactors with time (Set 6).....	40
Figure 5.14. The conductivity change in Z-Cote HP1-high IS set reactors with time (Set 6).....	41
Figure 5.15. The pH change in dispersion-acidic set reactors with time (Set 7).....	42
Figure 5.16. The Zn concentration change in dispersion-acidic set reactors with time (Set 7).....	42
Figure 5.17. The pH change in nano dispersion ZnO basic set reactors with time (Set 8).....	43
Figure 5.18. The Zn concentration change in dispersion basic set reactors with time (Set 8).....	44
Figure 5.19. The pH change in dispersion-high IS set reactors with time (Set 9).....	44
Figure 5.20. The Zn concentration change in dispersion-high IS set reactors with time (Set 9).....	45
Figure 5.21. The conductivity values of leachate in dispersion-high ionic strength set reactors	

with time (Set 9).....	46
Figure 5.22. Uncoated total (background + any nano Zn added) Zn mass (mg) in leachate.....	47
Figure 5.23. Z-Cote HP1 total (background + any nano Zn added) Zn mass (mg) in leachate.....	48
Figure 5.24. Dispersion total (background + any nano Zn added) Zn mass (mg) in leachate.....	48
Figure 5.25. Uncoated nano Zn mass in leachate (%).....	49
Figure 5.26. Z-Cote HP1 nano Zn mass in leachate (%).....	50
Figure 5.27. Dispersion nano Zn mass in leachate (%).....	51
Figure 5.28. Uncoated Nano- Zn mass retained in MSW (%).....	52
Figure 5.29. Z-Cote HP1 Nano- Zn mass retained in MSW (%).....	53
Figure 5.30. Dispersion Nano- Zn mass retained in MSW (%).....	54

LIST OF TABLES

Table 2.1. The properties of nanomaterials.....	3
Table 2.2. The application types of nanoparticles in different industrial sectors.....	5
Table 4.1. Properties of ZnO NPs that were used in the leaching experiments.....	20
Table 4.2. The equipment list for analyses and methodology.....	24
Table 4.3. The limit of detection of ions for Ion Chromatography (IC).....	26
Table 4.4. Digestion method for determination of Zn.....	26
Table 4.5. Microwave operating parameters.....	27
Table 4.6. The limit of detection (LOD) of metals for ICP-OES.....	27
Table 5.1. Characterization of Municipal Solid Waste.....	29
Table 5.2. Properties of each experimental set.....	31

LIST OF SYMBOLS/ABBREVIATIONS

Symbol	Explanation	Unit
ZnO	Zinc Oxide	mg/L
Cl ⁻	Chloride	mg/L
mM	Millimolar	mol/m ³
HNO ₃	Nitric Acid	
H ₂ SO ₄	Sulphuric Acid	
NaOH	Sodium Hydroxide	
HCl	Hydrochloric Acid	

Abbreviation	Explanation
Nanoparticle	NP
ENM	Engineered Nanomaterial
ISO	International Organization for Standardization
MSW	Municipal Solid Waste
WWTP	Wastewater Treatment Plant
CNTs	Carbon Nanotubes
ENM	Engineered Nanomaterial
ESEM	Environmental Scanning Electron Microscope
TS	Total Solids
VS	Volatile Solids
MC	Moisture Content
IS	Ionic Strength
COD	Chemical Oxygen Demand
TOC	Total Organic Carbon
TKN	Total Kjeldahl Nitrogen
IC	Ion Chromatography
TEM	Transmission Electron Microscopy
DGGE	Denaturing Gradient Gel Electrophoresis
SBR	Sequencing Batch Reactors
SRT	Sludge Retention Time
HRT	Hydraulic Retention Time
NOM	Natural Organic Matter

AOB	Ammonia Oxidizing-Bacteria
AAOB	Anaerobic Ammonia-Oxidizing Bacteria
NOB	Nitrite Oxidizing Bacteria
CANON	Completely Autotrophic Nitrogen Removal Over Nitrite
DLVO	Derjaguin-Landau-Verwey-Overbeek
EDL	Electrical Double Layer
OECD	Organisation for Economic Co-operation and Development

1. INTRODUCTION

The nanotechnology and nanoscience research areas have become one of the most important area in scientific researches (Park et al., 2016). The production of engineered nanomaterials (ENMs) has been increasing with each passing day. The value of nanomaterials in the global market was \$125 million in 2000 and based on the estimation it reached \$12.7 billion by 2008. The number of ENMs incorporated products has been reported as 1827 in 33 countries until today (Kwak et al. 2016).

This value is predicted to be \$30 billion by 2020 (Rodrigues, 2016). However, this increasing trend has also caused concerns about their effects on the environment and human health (Xiao-hong et al., 2015). Based on the Amara's Law the increase in production of ENPs is expected to originate a large number of nano-products and, therefore, nanowastes as shown in Figure 1.1 (Dwivedi et al., 2015).

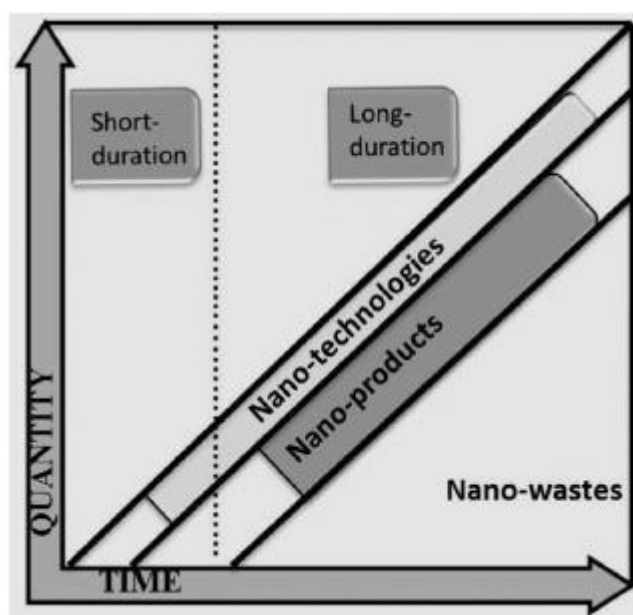


Figure 1.1. Relationship of ENPs growth over time (Amara's law correlation of nanotechnological growth) (Dwivedi et al., 2015).

Among these nanoparticles (NPs), silver (Ag), titanium dioxide (TiO_2) and zinc oxide (ZnO) are the major metallic elements commercially used (Yang et al., 2013). Nanoparticles are included in cosmetics, clothing, personal care products, electronics, coatings, and paints. TiO_2 is extensively used in manufacturing, cosmetic applications as a UV-absorber, food products, and environmental

remediation (Yang et al., 2013). In addition to excretion from humans, TiO_2 from sunscreens and paints is likely to be washed or disposed into sewage systems (Kiser et al., 2009). Ag NP is used as an antibacterial agent, SiO_2 as polishing and blinding agents, TiO_2 in solar cells and ZnO as UV-absorber in sun screen lotions. Furthermore, NPs are also used in filtration and purification, agricultural sector, aerospace and automotive (Keller et al., 2013a). It is estimated that the manufacturing of nanomaterials will increase from 1000 to 58000 tons yearly from 2011 to 2020 (Bolyard et al., 2013). In the long run, the production and use of nanoproducts will cause generation of increasing amount of waste including ENMs (Boldrin et al., 2014). Research activities about ENMs have mostly been carried out about the ecotoxicity of nanomaterials, but information about the fate and behavior of ENMs fate in the environment is lacking. Particularly, the research activities about the fate and behavior of ENMs in municipal solid waste (MSW) landfills and leachate are limited. Therefore, the main objective of this experimental study is to enrich the knowledge about the fate and behavior of ENMs in landfill and landfill leachate. Thus, within the scope of this experimental study, the leaching potential of zinc oxide (ZnO) NP was investigated using real municipal solid waste samples obtained from a landfill in batch reactor studies. ZnO NP is among the most commonly used ENMs in commercial applications; therefore, it has been selected for this study. Furthermore, the adverse impacts of ZnO NPs on biological waste treatment systems (such activated sludge wastewater treatment systems and anaerobic digestion of sewage sludge) have been recently reported as well. At the end of this study, it was expected to evaluate and determine the short-term behavior of ZnO NP within the MSW/leachate matrix.

2. LITERATURE REVIEW

2.1. Definition of Nanomaterials (NMs)

The definition of nano is indicated as a size ranging between 1-100 nm by International Organization for Standardization (ISO). As for nanomaterials, they are defined as materials having any external dimension in nano scale or internal or surface structure in nano scale (Dolez et al., 2015). Beyond this, nanoparticles are defined as a nano-object that has three external dimensions in nano scale (Boverhof et al. 2015). ENMs are also defined as anthropogenic in more than one dimension being as spherical, tubular, or irregularly shaped. They can aggregate or agglomerate in forms of organic, inorganic, crystalline, or amorphous structures (Weinberg et al. 2011). The key parameters of nanomaterials are their size, shape and morphological sub-structure (Brar et al. 2010). Nanoparticles have catalytic, electrical, magnetic, mechanical, optical, sterical and biological properties (Luther 2004). The basic properties of nanomaterials in detail are shown in Table 2.1 (Luther 2004).

Table 2.1. The properties of nanomaterials (Luther 2004).

Catalytic	Better catalytic efficiency through higher surface-to-volume ratio
Electrical	Increased electrical conductivity in ceramics and magnetic nanocomposites, increased electric resistance in metals
Magnetic	Increased magnetic coercivity up to a critical grain size, superparamagnetic behavior
Mechanical	Improved hardness and toughness of metals and alloys, ductility and superplasticity of ceramic
Optical	Spectral shift of optical absorption and fluorescence properties, increased quantum efficiency of semiconductor crystals
Sterical	Increased selectivity, hollow spheres for specific drug transportation and controlled release
Biological	Increased permeability through biological barriers (membranes, blood-brain barrier, etc.), improved biocompatibility

Nanoparticles comparatively larger surface area than the same amount of material. This specification might cause materials to be chemically more reactive. Their strength and electrical properties are affected as well. Moreover, the nano scale, below 50 nm, gives quantum effects to nano materials and provides optical, electrical and magnetic attitude other than the same material which is larger in size (OECD Report 2016).

The elements and compounds that are mainly applied as nanosizes to commercial products. These are classified as metals, oxide of metals, clays, carbon compounds. The examples of metals are iron, silver, gold, copper, nickel and aluminum, oxides of metals are iron, titanium, zirconium, aluminum and zinc; clays are talc, mica, smectite, asbestos, vermiculite, and montmorillonite, carbon compounds are fullerenes, nanotubes, and carbon fibers (Theodore and Kunz 2005).

Nanoparticles can be classified based on their dimensions, origins, chemistry and applications (Figure 2.1).

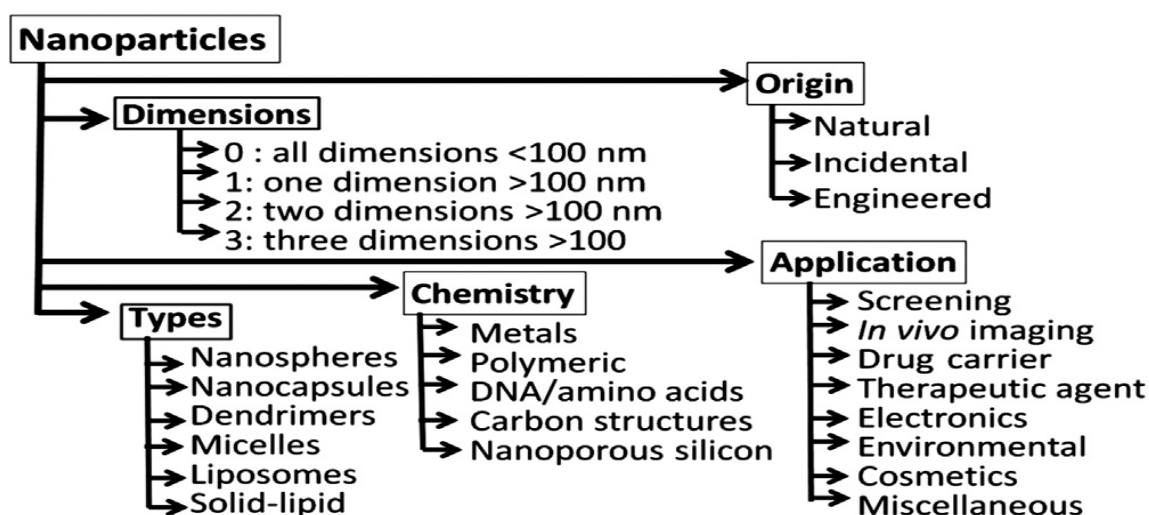


Figure 2.1. The classification of nanoparticles.

2.1.1. Application of Nanomaterials

The commercial application of nanomaterials has been increasing in various products because of their executive properties and functions (Kwak et al. 2016). There were about 1300 consumer products consisting of engineered nanoparticles in market by 2011 (Rodrigues 2016). Engineered nanomaterials are used in various sectors with different kind of applications. These sectors are; aerospace, automobile, chemicals, construction, cosmetics, electronics, energy, engineering, environment, food, household, medicine, military, security, sports, textiles (Dolez 2015). The application types of nanoparticles in different industrial sectors are demonstrated as an overview in Table 2.2. Nanoparticles have also been used commonly in water treatment processes. Metal oxide nanoparticles such as TiO_2 , ZnO and CeO_2 are used for the degradation of organic pollutants. High surface area and superior photolytic properties of metal oxide nanoparticles lead them to be preferred in water purification. In addition, they are used especially for removal of emerging contaminants in low concentrations. (Adeleye et al., 2016; Bethi et al., 2016).

Table 2.2. The application types of nanoparticles in different industrial sectors (Luther 2004).

Electronic, optoelectronic and magnetic applications	Biomedical, pharmaceutical and cosmetic applications	Energy, catalytic and structural applications
Chemical–mechanical polishing, Electroconductive coatings, Magnetic fluid seals and recording media, Multilayer capacitors, Optical fibers, Phosphors, Quantum optical devices	Antimicrobials, Biodetection and labeling, Biomagnetic separations, Drug delivery, MRI contrast agents, Orthopedics/implants, Sunscreens	Thermal spray coatings, Automotive catalyst, Membranes, Fuel cells, Photocatalysts, Propellants, Scratch-resistant coatings, Structural ceramics, Solar cells

Metallic nanoparticles are the most adjustable nanostructures having the synthetic control of their size, shape, structure, composition. They can be used as platform materials for biomolecular ultrasensitive detection, hyperthermal treatment for cancer, cell and protein labeling, and targeted delivery of therapeutic agents within the cells. However, metal oxides are beneficial with their unprecedented chemical properties such as their limited size and a high density of corner or edge surface sites. For example SiO₂ used for increase germination, alumina nanoparticles increases the root growth of plants and magnetic nanoparticles are applied in clinical use. Carbon nanotubes (CNTs) are commonly utilized in biological and biomedical applications. It is indicated in some reports, smart delivery system for the delivery of chosen molecules to the plant or animal cells are possible with CNTs. Also, yet another carbon nanoparticles example graphene oxide (GO) usage is increased in imaging agents, drug carries and tissue engineering materials (Subbenaik 2016).

ZnO NPs have been used in various products and areas such as plastic glass ceramics, paints, batteries, photocatalysis sensors, and solar cells; cosmetics, agriculture, medicine, drug-delivery due to their physical, optical and antimicrobial properties. (Sturikova et al., 2018; Wang et al., 2018; Sabir et al., 2014).

ZnO NPs are different from other metal oxides due to their increased surface area and transparency to visible light which makes them invisible when incorporated with other matrices (Theodore and Kunz 2005). The ZnO NPs have magnificent UV absorption and reflective properties. Thus, ZnO NPs are commonly used in most of the consumer products such as cosmetics, paints, coatings (Tan et al. 2015).

Likewise ZnO NPs, TiO₂ NPs are also used in sunscreens as absorbents the light as well (Luther 2004).

2.2. Behavior of Nano-ZnO in the Environment

The rapid increase in commercial use of ENMs has caused concerns about their material flows in the environment (Brar et al., 2010). Nanoparticles are expected to exhibit different transportation potentials and behavior of them might substantially differ in the environment because of the differences in the processes (Sweet et al., 2006; Goswami et al., 2017). They are most likely insoluble in water, but some modifications of surface chemistry might alter their water solubility. Thus, their fate, transport and behavior in the environment would change (Sweet et al., 2006). Although the use of NPs has many commercial benefits, their environmental implications are still unknown (Keller et al. 2013a).

The potential nanoemission ways of nanomaterials to the environment are described as production, use and end-of-life phases and the release of ENMs might be from any stage of their life cycle such as production, storage, transportation or disposal points (Caballero-Guzman et al., 2016; Part et al., 2018). Incineration or recycling processes are examples for release during waste management process. In the end, the ultimate phases of their life most probably are landfills or sediments if they are not in the recycling processes (Caballero-Guzman et al., 2016).

In order to advance a sustainable approach to nanotechnology, it is essential to understand and regulate the risk assessment of ENMs by taking into consideration exposure and possible hazards of them (Caballero-Guzman et al., 2016). Thus, a number of studies about environmental release models and exposure of ENMs have been performed during recent years.

Figure 2.2 basically shows how and in which stage ENMs are released to the environment. Based on the diagram, the release occurs via two stages. One of them is nanoproduct or ENM release in handling processes which are shown as dark blue arrows. These are ENM production, nano-application manufacturing, nano-application use and disposal processes. The other stages create the final transfers to the environment which are also seen as light blue arrows. The potential release of ENMs during usage process is predicted to be higher because the control procedures are lesser in this process. Hence, larger releases are possible to be transported to the environment directly (Caballero-Guzman et al., 2016).

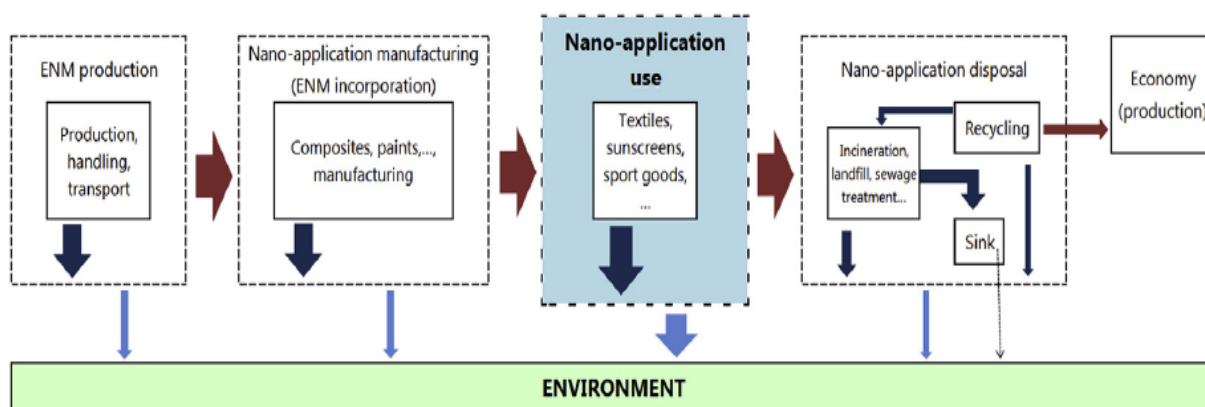


Figure 2.2. The release of ENMs during their life cycle (Caballero-Guzman et al., 2016).

Keller et al. estimated the emissions of ENMs according to releases during manufacturing, using and disposal for the global flow of ENMs through the world economy for the top 10 ENMs (Figure 2.3). The estimates were done assuming the high production in 2010 and high emission assumptions during their life cycle (Keller et al., 2013a).

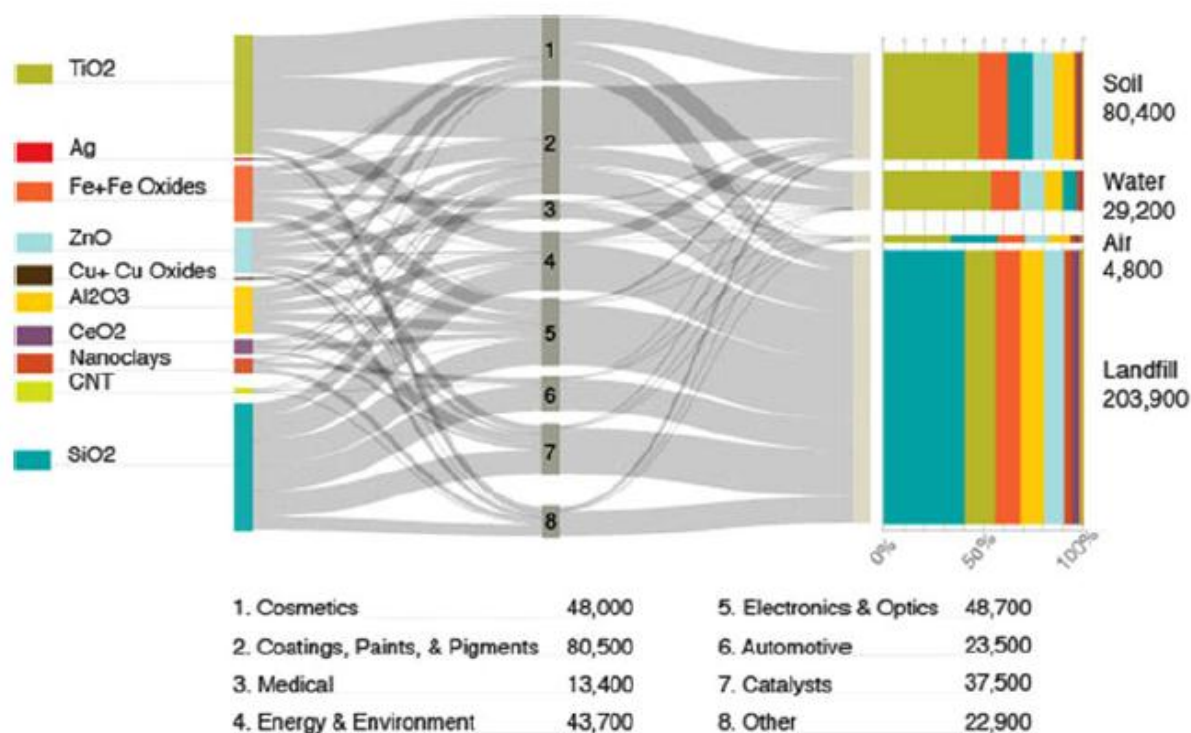


Figure 2.3. Global flow of ENMs in 2010 (Keller et al., 2013a).

According to data shown in Figure 2.4, it was estimated that most of ZnO ENMs would be used in medicine, cosmetics, electronics and optics, coatings, paints and pigment products and annual production of ZnO as of 2010 would be more than 30,000 metric tons. It was also estimated

that the highest emissions were from use of ZnO ENMs as cosmetic products, which might pass through the Waste Water Treatment Plants (WWTPs). Overall estimated emissions were 90–578 tons/year to the atmosphere, 170–2,985 tons/year to receiving water bodies, and 3,100–9,283 tons/year to soils. In addition, it was also estimated that 21,153–28,171 tons/year were disposed of in landfills (Keller et al., 2013a).

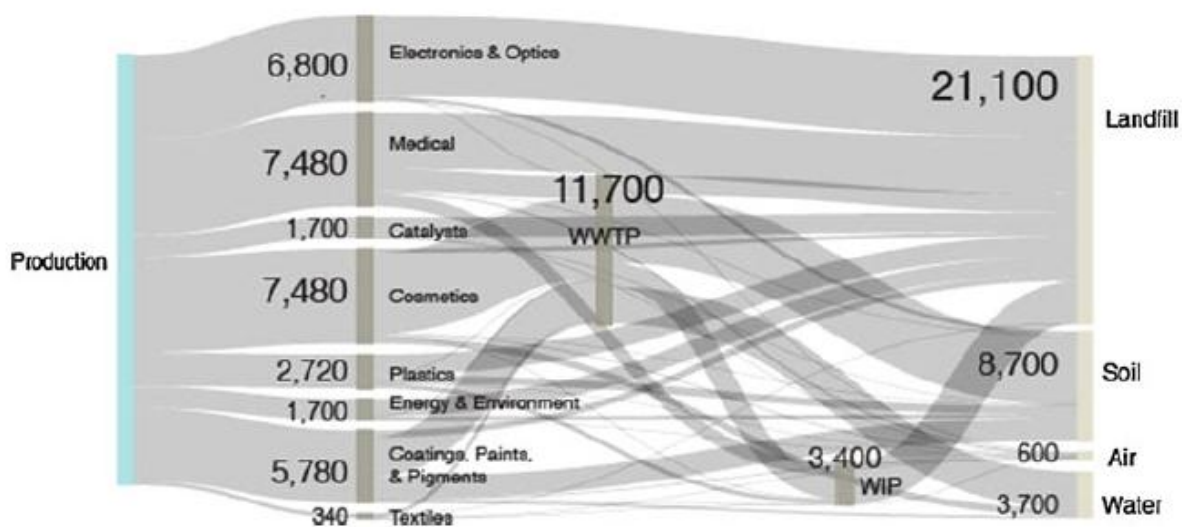


Figure 2.4. Global material flows for ZnO ENMs (metric tons/year) in 2010 (Keller et al., 2013a).

According to Keller et al., these estimated releases of ENMs into multiple environmental zones can be used for quantifying mass loadings and also identifying environmentally concerned applications. Most of the ENMs ended up in landfills with higher amounts than the high production and emission scenario. The most common type of applicants such as coatings, paints and pigments had the highest probability of being released into soil and water. At present, around 63–91 % of ENMs are eventually disposed of in landfills. WWTPs have an important way to be transferred of ENMs to soil and water (Keller et al., 2013b).

The knowledge of the fate of nanomaterials in waste management and recycling process is still insufficient (Caballero-Guzman et al., 2015). The authors studied the flow models of certain nanomaterials, nano-TiO₂, nano-Zn, nano-Ag and CNT, in recycling system in Switzerland. According to the results obtained, the ENMs are not transmitted to the new materials via recycling process substantially. The larger percentage of ENMs moves in the cycle as wastes and then passes to incineration and landfills. There goes diminished fraction of ENMs to products in some industries.

Boldrin et al. proposed a framework for environmental exposure assessment for nanoparticles in solid phase by working on 5 steps such as quantification of nanowaste amounts, evaluation of matrix properties and nanowaste treatment processes, evaluation of the nanostructure's physicochemical properties, evaluation of transformation processes and release of ENMs into the environment and assessment of potential exposure using three selected products, nanosilver polyester textile, nano TiO₂ sunscreen lotion and carbon nanotube tennis racquets. It was stated that the exposure of nanomaterials through the waste stream became urgent with the rapid increase of using nanomaterial in products. In combustion processes, flue gas cleaning technologies need to be investigated more entirely with respect to variety of ENM types and subsequent releases such as bottom ash should be considered. In landfilling processes, it should be considered how physicochemical and hydraulic conditions might have effects on both the matrix material and the transformation on the ENMs themselves (Boldrin et al., 2014).

It is stated in literature that it is difficult to predict the behavior of natural nanoparticles (Caballero-Guzman et al., 2016). All along the processes, they go through conversions and released ENMs might behave other than natural nanoparticles. The inadequacy in detection of ENMs in the environment borders exposure assessments for researchers. The low concentrations of ENMs and complexity of their origins may cause to differ natural and ENMs from each other. It is indicated that ENMs are not released as a single particular. They may also be released to the environment as an ingredient of commercial products. The researches on the ENMs exposure modeling are insufficient compared with other nanomaterial exposure modeling studies (Caballero-Guzman et al., 2016).

The behavior of released ENPs depends on the characteristics of both the environment and themselves. The behavior of ENPs might be altered in the environment due to abiotic and biotic impacts such as soil and water quality parameters or biomass and microorganisms (Dwivedi et al., 2015). Abiotic factors which have an influence on their mobility are pH, ionic strength, particle surface chemistry, interactions of nanoparticles with other pollutants and natural organic molecules. The fate, transport, behavior and ecotoxicology in the aquatic environment is controlled by their inherent specifications especially their surface energy and stability (Omar et al., 2014).

After being released into the atmosphere, they act like an aerosol, moving some distance from the release point and eventually delivering to the soil or water. In the water form, they tend to aggregate and precipitate based on features of ENMs and water conditions. The altered ENMs are transferred through the soil flow to groundwater. Herein, there are some parameters that cause to

ENMs being hold in soil matrix. These parameters that lead to the transport of ENMs are essentially, pH, ionic strength, zeta potential and texture of the soil. Particularly, pH and ionic strength affect aggregation strongly. In consideration of these circumstances, aggregation, deposition and stabilization of ENMs arise. It is also stated that the adsorption of ENMs on the surface of soil minerals might decelerate their transportation. This sorption is hinged on the surface charge of ENMs and occurrence of soil minerals. There exist a few nanomaterials having higher leaching capability to groundwater as a potential contaminant (Pachapur et al., 2015; Dwivedi et al., 2014).

The surface potential of NPs also affects their stability and aggregation. High negative surface potential tends to stabilize NPs while low negative surface potential leads to aggregation of NPs. Surface charge, particle size, ionic strength, pH and cation composition of the solution, and particle shape dominate aggregation (Batley et al., 2013).

Yeskechel et al. investigated the transport behavior of three common nanoparticles, Au, Ag and ZnO, in partially saturated sand columns. The authors considered initial ENP concentration, saturation level and background solutions and their effects on their mobility and retardation. The Au and Ag NPs were citrate-stabilized, ZnO NPs were positively charged. The results demonstrated that the negatively charged nanoparticles Au and Ag exhibited high mobility through the partially saturated sand column. The behavior of Ag NPs was lightly affected by nanoparticle concentration and saturation rate. But high concentration of CaCl_2 decreased the movement of Ag NPs. Conversely, the ZnO NPs were utterly stayed in the column due to the electrostatic interactions of positively charged of their surfaces. Humic acid decreased the mobility of Au and Ag nanoparticles and on the contrary, it increased the mobility ZnO NPs. The existence of humic acid altered the surface of ZnO NP from positive to negative thus their mobility increased. Based on these results, it is stated that the transport and fate of the nanoparticles in partially saturated area is heavily influenced by chemical structure of the environment (Yeskechel et al., 2016)

The effect of ionic strength and cation valence on the transport and deposition kinetics of ZnO NP in saturated porous media was studied by Jiang et al. (2012). Under different concentrations of NaCl and CaCl_2 were used in packed columns. They found out that the ion strength and valance directly affected the transportation kinetics of ZnO. The increase in solution ionic strength led increase in deposition of quartz sand. The divalent ions also improved the deposition (Jiang et al., (2012).

2.2.1. Behavior of Nano-ZnO in Landfills

It is estimated that 63–91 % of over 260,000–309,000 metric tons of global ENM production in 2010 ended up in landfills (Keller et al., 2013a). According to Reinhart et al. (2010), 50% of the nanomaterials produced worldwide end up in landfills. Nanomaterials are listed as emerging contaminants in landfill leachate and the fate of these emerging materials in landfills is not yet understood (Ramakrishnan et al., 2015). There exist many researches regarding the impact of landfill leachate on ENMs stability and mobility. However, the release and transfer processes of ENMs from solid waste to leachate are still not yet known entirely (Part et al., 2018).

One of the most relevant researches in this area is about the fate of coated zinc oxide (ZnO) NPs in landfills. In this study, the authors examined the possible transport mechanisms of ZnO (coated) NP within landfills and inhibitory effects on anaerobic and aerobic processes. It was found out that the ZnO NPs did not pose any inhibition effect due to their low concentration (Bolyard et al., 2011).

Another study, which covered the modeling of flow of ENMs during waste handling, was conducted by Mueller et al. In this study, the authors focused on nano-silver (Ag), nano-TiO₂ and Carbon Nano Tubes (CNT) NPs. This study showed that a significant amount of NPs would end up in landfills. The authors also stated that the nano-ZnO, nano-TiO₂ and nano Ag might reach to landfills in incineration bottom ash (Mueller et al., 2013).

The behavior and fate of NPs in landfill leachate was investigated by Bolyard et al. The focus of the research was to figure out the effect of three selected nanoparticles, namely ZnO, TiO₂ and Ag, on biological landfill processes and the form of Zn, Ti and Ag in leachate. Each NP was added to the real leachate samples that were classified as middle-aged and mature leachate. It was indicated that NPs did not affect the biological activity taking place in leachate. It was also stated that it was difficult to estimate the mobility of NPs in a landfill environment due to the heterogeneity of landfill leachate and the variation in NP characteristics (Bolyard et al., 2013).

Leaching potential of NPs outside the landfill will differ depending on the characterization of nanomaterial, characterization of the waste containing nanomaterials, physico-chemical and hydraulic properties and operation methods of the landfill. Consequently, the behavior and leaching potential of NPs depend on different parameters and their leaching potential has not been clearly stated until now (Nowack et al., 2012; Boldrin et al., 2014). In addition, Reinhart et al. also stated

that the parameters such as leachate characteristics, moisture content, and temperature should be considered in order to determine the fate of NPs in landfills (Reinhart et al., 2010).

Keller et al. studied the exposure of ENM from global to regional to local using predicted releases data of 10 major ENMs. The authors focused on the quantity of ENM releases to water, air and soil at local level firstly. The releases of ENM to air, water and soil were expected to be 0.1-2 %. Therefore, the release during production was between 98-99 %. The population of each region and the development level of countries were considered for prediction. Based on the estimated exposure of ENMs research 60-86 % of ENMs in electronics, automotive and solar panels might end up their life cycle in landfills. Additionally, the authors stated that the personal care products such as sunscreens and cosmetics, coatings, paintings and pigments were expected to enrich exposures to air, water and soil after electronics, automotive and solar panels. Furthermore, it is also indicated that high releases to air, water and soil mean less ENM concentrations in landfills (Keller et al., 2013b).

In a relatively recent work, Dulger et al. investigated the leaching potential of nano-TiO₂ in fresh real MSW and synthetic MSW with batch experiments. Batch reactors containing MSW were spiked with nano-TiO₂ solutions, which were prepared with different concentrations. The reactors were operated under acidic, basic and high ionic strength conditions. The experiments showed that a high concentration of nano-TiO₂ remained in the solid waste rather than remaining within the leachate. Ti concentration in leachate decreased during 12 h rapidly and after 12 h exhibited a stable tendency. It was stated that although Ti concentrations decreased in acidic condition tests more rapidly, there was not a significant effect of acidic, basic and ionic strength conditions on nano-TiO₂ leaching potential. Environmental Scanning Electron Microscope (ESEM) analysis that was performed using synthetic waste also showed that the nano-TiO₂ tended to aggregate on the waste surface. It was also stated that the solid waste composition was complex and variable, thus the results might differ. The results indicate that solid waste has a higher potential to retain nano-TiO₂ and further long-term tests are needed (Dulger et al., 2016).

Demirel discussed the impacts of NPs on anaerobic digestion processes. It was emphasized that most of the ENMs ended mostly in wastewater treatment systems, landfills or incineration plants. Since anaerobic digestion is a common way of treatment process with gaining energy (biogas) and ENMs are classified as emerging contaminants, the effects of nanomaterials in the anaerobic digestion system have become crucial. Various metal oxide nanoparticles such as CuO, ZnO, CeO₂ and Ag were discussed. It was reported that CuO, ZnO, and CeO₂ adversely affected the biological

activity based on the concentration. The high concentration of nano Ag also had an adverse impact on biogas production from landfill. CuO NPs exhibited more adverse impact on biological activity, when compared with ZnO NPs, even at lower concentrations (Demirel 2016).

Very recently, another research about the long term effects of ZnO NPs on waste stabilization and biogas production in simulated landfills was conducted by Temizel et al. The authors performed experiments using two simulated conventional and bioreactor landfills. 100 mg nano-ZnO/kg of dry waste was added to the reactors. Each reactor was operated with real MSW samples at 35 °C for almost 1 year. The authors focused on the observation of daily biogas production, the composition of gas and leachate Zn concentration. The results obtained from this experimental work showed that the ZnO NPs caused a decrease about 15% the production of biogas in nano-ZnO added reactors compared to control reactors. Apparently, there was a minor inhibitory effect of nano-ZnO on biogas generation. It was assumed that as Zn^{2+} that released from nano-ZnO might have affected the methanogenic Archaea activity negatively during the methanogenic phase. However, waste stabilization was faster in bioreactor landfills than conventional landfill reactors due to the recirculation of leachate in bioreactor landfills. Organic matter degradation was also faster in bioreactor landfills with respect to gas production. There was no significant difference in Zn leachate concentrations although the same amount of nano-ZnO was added to both types of reactors (Temizel et al., 2017).

2.2.2. Behavior of Nano-ZnO in Wastewater Treatment

In recent years, the adverse effects of ZnO NPs on biological treatment processes have become more of an issue and researches have also focused on this. The researches based on this issue are summarized below briefly.

The NPs that are daily used in household and industrial commodities will find their way especially through waste disposal routes into wastewater treatment facilities and end up in wastewater sludge eventually (Brar et al., 2010; Choi et al., 2017). The production and use of ZnO NPs increase rapidly day after day hence the concentration of them in the environment also increases inescapably. The expected rate of increase in sludge-treated soil is about 1.6-3.3 $\mu\text{g}/\text{kg}/\text{yr}$ and this ratio would be in mg/L in near future (Tan et al., 2015).

The transported nanoparticles from wastewater treatment plants to the aquifer are predicted to be about 26-39% of the total (Choi et al., 2017).

The existence of ZnO NPs can have inhibitory effects on biological nutrient removal in wastewater treatment facilities. Hence, they have been described as one of the most toxic nanomaterials. Activated sludge processes are applied in most of the wastewater treatment plants and the bacteria are in these processes degrade organic matter. However, the bacteria are very susceptible to toxic compounds and ZnO NPs may inhibit bacterial activities due to their antibacterial characteristic (Hou et al., 2014; Tan et al., 2015; Chaúque et al., 2014).

Several studies asserted that ENMs in wastewater treatment facilities end in activated sludge rather than flowing through the effluent and release to the environment (Chaúque et al., 2014; Puay et al., 2014).

Puay et al. investigated the effects of ZnO NPs on the bacterial community with simulating biological wastewater treatment plant using sequencing batch reactors (SBR) in a lab-scale work. The SBR was operated with 16 days of sludge retention time (SRT) and 11.7 hours of hydraulic retention time (HRT). In order to reach a steady-state, the SBR was performed up to 56 days and as from 57th day; the system was operated with 1 mg/L ZnO to provide a simulated condition correspond to environmental concentrations. The SBRs were operated up to 56 days for steady-state, on the 57th day the system exposure with 1 mg/L ZnO. It was found that the ZnO NPs had an adverse effect on nitrogen and phosphorus removal prominently; on the contrary, they did not affect chemical oxygen demand (COD) removal severely. The effects of ZnO NPs on the bacterial community were analyzed using Denaturing Gradient Gel Electrophoresis (DGGE) finger patterns and cluster analysis. The results showed that ZnO NPs affected the bacterial community structure. The fate of nano-ZnO was observed in three phases and it was found that removal of Zn from wastewater changed with Zn absorption onto activated sludge. The main removal way of ZnO from wastewater was absorption and it was suggested that safe handling and disposal of ZnO NPs-enriched sludge should be investigated (Puay et al., 2014).

Chaúque et al. studied the influences of the physicochemical changes such as pH and ionic strength on the stability of ZnO NPs in domestic wastewater to understand the fate and behavior of them in wastewater treatment processes and potential releases to the environment if they are untreated in the effluent. The authors also investigated the agglomeration images of ZnO NPs in both wastewater and deionized water by transmission electron microscopy (TEM). The results showed that in aqueous environment, pH, ionic strength and other sort of electrolytes had an impact on the stabilization of nano-ZnO. The high pH and ionic strength caused a decrease in Zn concentration in filtrate. The release of Zn was more notable under acidic and high ionic strength

conditions. In addition, Zn concentration in wastewater was lower than the concentration in deionized water. The presence of biomass in wastewater could be the reason of the low Zn concentration. These findings reveal that the removal of ZnO is probably via the abiotic, biosorption and biosolid mechanisms because of the deposition of NPs in sludge. It is stated that the way of ZnO NPs through the environment from wastewater is presumably the handling of sludge. Therefore, the use of sludge in agricultural activities and fly ash from incineration of sludge process are the release pathways of ZnO NPs (Chaúque et al., 2014).

Another research was also performed about the fate and behavior of ZnO NPs in a simulated wastewater treatment plant (WWTP) by Chaúque et al. The authors focused on three points; the fate of ZnO NPs in a simulated WWTP according with OECD 303 A guideline, examining the transformation of ZnO NPs from influent to effluent in the system and exploring the effects of ZnO NPs concentration on organic matter degradation. It was revealed by the authors that remarkable concentration of ZnO NPs was removed from wastewater and only a little portion of it was released to the environment via wastewater treatment facilities. However, considerable portion of ZnO NPs remained in wastewater sludge (Chaúque et al., 2016).

2.2.3. Toxicity of Nano-ZnO

The rapid increase in usage of ENMs in commercial products and industry has also raised concerns about their toxicity. The application of ZnO NPs is in the third order among metallic nanoparticles. The discharge of ZnO NPs through water after reaching considerable amount may cause adverse effects on algae and microflora. It also inhibits the photosynthetic activity of bacteria and transformation of structures between microbial communities (Xu et al., 2015).

The physical and chemical properties of ZnO NPs have influences on its toxicity. The toxicity mechanism was mostly affected by its particle size, surface coating, exposure mode, time, pH and temperature. These properties have different effects on different kind of species (Hou et al., 2018). For instance, ZnO NPs coated with oleic acid (OA) and poly (methylacrylic acid) (PMAA) were less toxic than uncoated ZnO NPs since surface coatings cause a decrease in toxicity (Garner and Keller 2014).

ZnO NPs have the highest capacity of toxicity among the other metal oxide nanoparticles such as TiO₂, SiO₂, CuO. It is crucial to understand the effects of the toxicity mechanism in detail. The dissolution of ZnO NPs is one of the major reasons of its toxicity. If the particle dissolution occurs

partially, not completely, toxicity effect is observed due to the high toxicity of dissolved zinc ions. Particle dissolution depends on inherent physico-chemical properties such as particle size surface area, chemical composition and environmental conditions such as pH, temperature, organic matter. These conditions and properties all together have an influence on the toxicity degree of ZnO NPs. Acidic conditions increase the toxicity due to the dissolution of ZnO NPs. Also, temperature decrease originates lower solubility cause a decrease in the toxicity. It is also indicated that free ion concentrations have a significant effect on toxicity. If the concentration of ZnO NPs reaches to the sufficient level, the risk of them to environmental biota should be considered (Ma et al., 2012).

Nano ZnO also shows considerable antibacterial activities over a wide spectrum of bacterial species. Nano ZnO can enter inside the cell interacting with bacterial surface or core and shows bactericidal activity. Accordingly, ZnO NPs are toxic to bacteria (Sirelkhatim et al., 2015).

For instance, recently Wang et al. investigated the causes of six different metal oxide nanoparticles toxicity mechanism with focusing on whether the toxicity comes from solely the nanoparticles, the ions or combination of both. They also analyzed the inhibition of metal oxide NP's on bioluminescence of *Photobacterium phosphoreum*. It is indicated that the metal oxide NPs and their dissolved metal ions are included in three phases, dissolution, adsorption and hydrolysis. The results exhibited clearly that the ZnO NPs had the highest antibacterial activity on *Photobacterium phosphoreum* and the dissolution of ZnO was substantially higher than those of the other NPs. It can also be inferred that the antibacterial effect of ZnO occurs with released Zn^{2+} (Wang et al., 2016).

The effects of ZnO NPs on microbial activity and microbial community of completely autotrophic nitrogen removal over nitrite (CANON) process in a membrane bioreactor was investigated. In CANON process, ammonia-oxidizing bacteria (AOB), anaerobic ammonia-oxidizing bacteria (AAOB) and nitrite oxidizing bacteria (NOB) play a crucial role on oxidizing and conversion steps. The authors aimed to ascertain the effects of ZnO NPs on microbial activity and nitrogen removal and the evolution of microbial community under ZnO NPs. The results revealed that ZnO NPs had a substantial effect on CANON process. It was found that low ZnO concentration (≤ 5 mg/L) was beneficial for bioactivity, nitrogen removal, microbial biodiversity and stability of CANON process. ZnO concentration achieved the best improvement at 1 mg/L level. On the other hand, both AOB and AAOB were suppressed and there occurred a decrease in nitrogen retention removal rate when ZnO concentration reached to 10mg/L. As a result, it is

indicated that long term exposure of ZnO NP had an adverse effect on the microbial diversity (Zhang et al., 2017).

Another research about the comparison of the effects Zn NPs, ZnO NPs and Zn ions on nitrifying bacterial community was studied by Wu et al. The results revealed that at low Zn concentration (0.1 mg/L), the nitrification rate was raised by Zn ions rather than Zn and ZnO NPs themselves. However, under high Zn concentrations Zn ions were more toxic than Zn NPs (Wu et al., 2018). It can be inferred from these researches, the toxicity of ZnO NPs and Zn ions might have positive or negative effects with the concentration level.

3. STATEMENT OF THE PROBLEM

The increase in the production of nanomaterial incorporated consumer products has raised the concerns about their fate, behavior and transport in the environment. Since their ultimate points of life cycle are wastewater treatment facilities, recycling processes and landfills, scientists have focused on the behavior of ENMs in waste management systems. There exist various research activities about their transport and behavior in wastewater treatment systems, such as activated sludge wastewater treatment and anaerobic digestion of sewage sludge systems. However, there is a considerable lack of knowledge about the fate and transport of ENMs in MSW landfills and landfill leachate. This laboratory-scale research has aimed to investigate and compare the leaching behavior of different kinds of ZnO NPs in real municipal solid waste samples under different environmental conditions using batch tests. Therefore, the main objective of this study was primarily to determine the short-term behavior and fate of different types of ZnO within the MSW-leachate matrix in batch reactors.

4. MATERIALS AND METHODS

4.1. Preparation and Characterization of the Solid Waste

In the experiments, real MSW samples obtained from İZAYDAŞ İzmit landfill site were used in order to investigate the leaching behavior of nano-ZnO. The composition of İzmit İZAYDAŞ municipal solid waste (MSW) is given in Figure 4.1 (This information was provided by İZAYDAŞ Plant, personal communication).

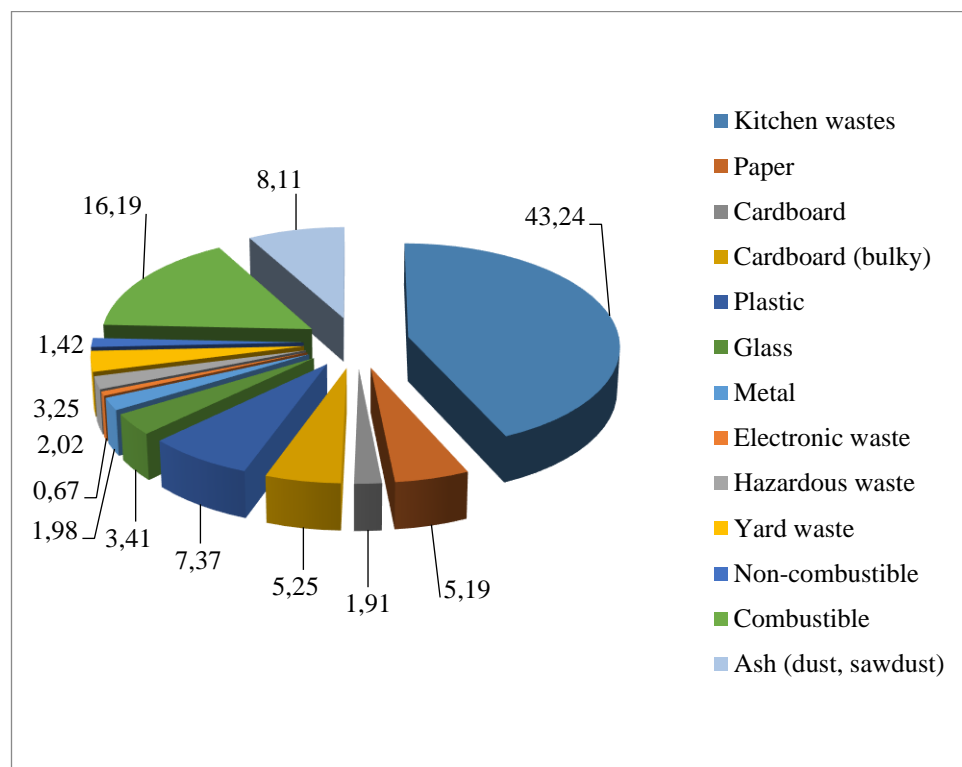


Figure 4.1. Components of İzmit İZAYDAŞ MSW.

İZAYDAŞ is a sanitary landfill plant established in 1996 and it is located near İzmit, Kocaeli. It has interim storage areas, hospital and hazardous waste incineration plants, excavation areas, hospital waste sterilization plant and biogas plant units. Municipal solid waste capacity is 3.163.000 m³. For the experiments, shredded, homogeneously mixed fresh MSW samples about 10 kg were taken from İZAYDAŞ and stored at 4°C prior to use. Solids, moisture content and metal analysis of MSW were performed in order to determine the background properties before leaching tests. Solid waste samples were selected as they could represent the content of MSW uniformly. All of the solid waste samples collected from İZAYDAŞ were spread on the ground and divided into eight compartments. Then, samples of equal weight (w/w) were taken from each of the compartment.

This representative sample was used to determine the background characterization of the MSW. The representative sample was dried to analyze moisture content. The dried sample was also pounded into dust and 0.15 g sample was used for microwave acid digestion method to analyze the initial total metal content of the MSW. Detailed characterization experiments were conducted to determine background characteristics. Total solids, heavy metal, pH, conductivity, TOC, IC, COD and TKN analyses were carried out for chemical characterization of the real MSW sample. In addition, an eluate was prepared in order to analyze certain characterization parameters. The eluate was prepared based on total solid content of solid waste sample. IC, TOC, COD and TKN experiments were conducted using the eluate.

4.2. Preparation of ZnO stock solution

In total, 3 different commercial nano ZnO were used for leaching experiments. Uncoated, Z-Cote HP1 and dispersion ZnO NPs obtained from different commercial brands were used for this experimental work (Table 4.1).

Z-Cote HP1 and uncoated powder nano ZnO were added to the batch reactors in solution. Before each experimental set, a new fresh 100 mg/L ZnO stock solution was prepared. 100 mg nano powder ZnO was added to 1 L of deionized (DI) water and the mixture was located in an ultrasonication bath for 30 minutes to provide homogeneous mixing. In order to prevent losing any remaining part in a beaker, this sonification step was repeated for at least three times (Weir 2011).

Table 4.1. Properties of ZnO NPs that were used in the leaching experiments.

NP	ZnO (uncoated)	ZnO (coated)	ZnO (slurry)
Brand	Sigma Aldrich	BASF	Sigma Aldrich
Commercial Name	Zinc oxide	Zinc oxide, Triethoxycaprylylsilane (Z- COTE HP1)	Zinc oxide
Shape	Powder (nanopowder)	Powder (hydrophobic)	Dispersion
Particle Size	<100 nm	<200 nm	<100 nm

The particle size and shape of uncoated and Z-COTE HP1 ZnO NPs were also analyzed using Environmental Scanning Electron Microscope (ESEM) at Boğaziçi University. The surface of the each sample was coated using Sputter Coating (Quorum Technologies, UK) device before ESEM analysis. The ESEM images of nano-ZnO are shown in Figures 4.2, 4.3 and 4.4, respectively

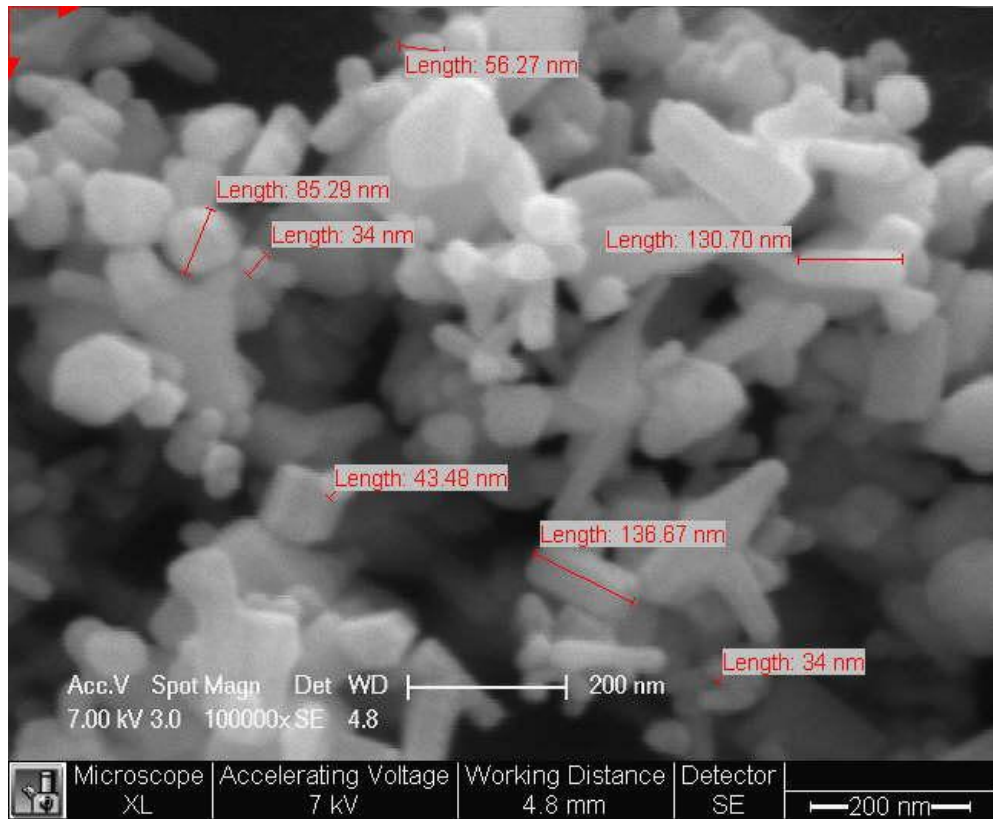


Figure 4.2. The average particle size of uncoated nano-ZnO.

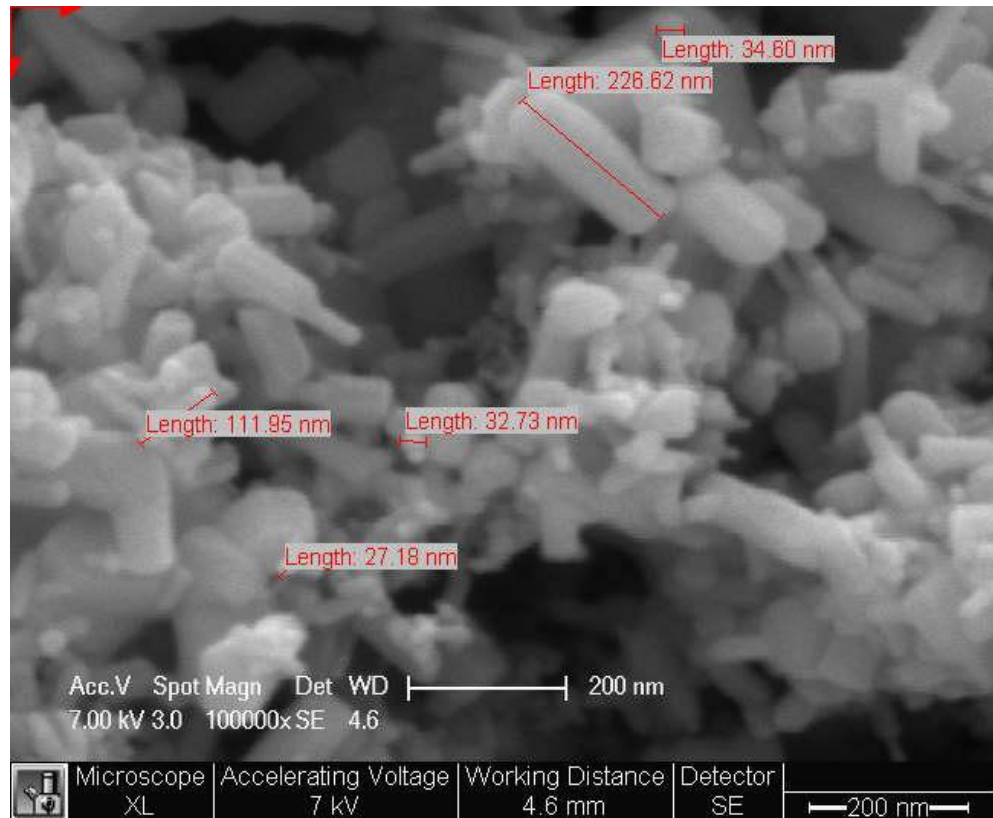


Figure 4.3. The average particle size of Z-Cote HP1 (coated) nano-ZnO.

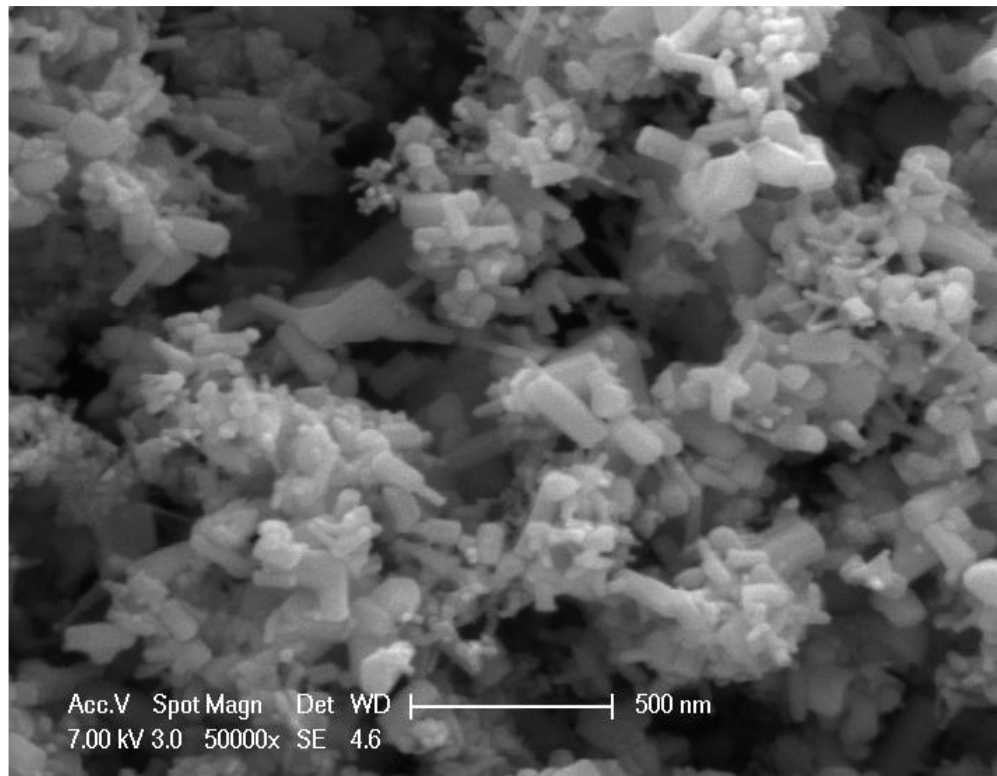


Figure 4.4. The ESEM image Z-Cote HP 1 (coated) nano-ZnO.

4.3. Batch Reactors Design and Operation

1 L of glass bottles were used to conduct leaching experiments as batch reactors. The batch reactors were loaded with different concentration of nano-ZnO stock solution as 0 (control reactor), 10, 25 and 100 mg/L. Each reactor was prepared with 250 g of fresh and shredded municipal solid waste (on wet weight basis), which was taken from İZAYDAŞ plant. After loading of fresh solid waste to the reactors, 300 mL of stock solution with various concentrations of nano ZnO were loaded to the batch reactors. The batch reactors were shaken by WiseShake SHR-2D (Wise Laboratory Instruments) after loading with three different types of ZnO NPs for three days (72 hours) to attain steady-state conditions (Figure 4.5). The batch reactors were operated under acidic, basic and high ionic strength (IS) conditions to understand the behavior of nano-Zn under different environmental conditions. It was determined to adjust the initial pH range to 5-6 for acidic sets and 12-13 for basic sets. 1-2 mL of 6 N H₂SO₄ and 15-20 mL of 1 N NaOH solutions were used to adjust acidic and basic conditions in the batch reactors, respectively. The pH condition in batch reactors tended to be at very low values and decreased rapidly after the experiments began. Therefore, the pH for basic condition reactors was held at very high values in the beginning of the experiments in order to supply a basic environment during the rest of the experimental period. The ionic strength (IS) was determined to be 35 mM for high ionic strength sets. In order to increase the

ionic strength, 0.6 g/L NaCl was dissolved in the solution. Thus, the IS of the leachate was reduplicated, from 35 to 70 mM (Sakallioğlu et al., 2016). During the experiments, no MSW sample was taken from the reactors. 10 mL of leachate samples were regularly withdrawn from batch reactors at pre-determined time intervals and they were analyzed for Zn concentration, pH, conductivity and particle size distribution. In total, 13 leachate samples were taken at 0., 1., 2., 3., 4., 5., 6., 12., 24., 36., 48., 60. and 72nd hours. Also, no additional moisture was added to the reactors not to dilute the system during the sampling process as well.



Figure 4.5. Batch reactors in shaker.

4.4. Analytical Methods

4.4.1. Experimental Analyses

The pH and conductivity equipment were embedded into batch reactors in order to measure pH and conductivity at pre-determined time intervals. The leaching tests were aimed to ascertain the Zn concentrations of samples taken at pre-determined time intervals. The samples were digested with microwave assisted digestion method substantially, total Zn were determined with Inductively Coupled Plasma-Optical Emission Spectrophotometry (ICP-OES). The experimental methods and the equipment that were used for the characterization and leaching tests are summarized in Table 4.2.

Table 4.2. The equipment list for analyses and methodology.

Name/Model	Aim	Method
COD digester	COD	5220 D Method Closed Reflux, Colorimetric (APHA, AWWA, WPCF,1998)
Perkin Elmer AAS	Determination of Alkali and Heavy Metals	ASTM 3010
Perkin Elmer ICP-OES	Determination of Heavy and Trace Metals (Ti, Zn, Si, Ag)	TS EN – ISO 11885
Nuve Oven	Determination of Solid Waste TS, VS and MC	2540 Method (APHA, AWWA, WPCF, 1998)
Sartorius Precision Balance	Determination of Solid Waste TS and MC	2540 Method (APHA, AWWA, WPCF, 1998)
WTW Conductivity Meter	Conductivity	Standard Method
Hanna Instruments HI 221	pH	Standard Method
Dionex ICS-3000 Ion Chromatography	Determination of Ions	SM 4110
HACH Digesdahl Digestion Apparatus, 115 Vac	Determination of Total Kjeldahl Nitrogen	HACH Method 8075
HACH Portable Data logging Spectrophotometer	Spectrophotometer	HACH Methods
Shimadzu TOC-V Total Organic Carbon Analyzer	Determination of Total Organic Carbon	Standard Method
WiseShake SHR-2D (Wise Laboratory Instruments)	Shaking batch reactors	-
Bandelin Sonorex	Ultrasonication	-
Brookhaven 90 Plus	Particle Size Analysis	-

The following measurements were conducted throughout the study.

4.4.1.1. Total Solid (TS) and Volatile Solid (VS). Total solids and moisture content measurements were conducted according to Standard Methods as stated above (Table 4.5). The sample was weighed before drying and it was dried at oven at 103 °C for 1 hour. After drying, the sample was put in a desiccator to cool to room temperature. After cooling, the sample was weighed again. The difference before and after drying indicates the moisture content of MSW. The sample was put in a muffle furnace at 550 °C for minutes. After taking from muffle furnace it was weighed again and the difference showed volatile solid.

4.4.1.2. Chemical Oxygen Demand (COD) Analysis. The chemical oxygen demand (COD) is commonly used to measure indirectly organic compounds in water. The dichromate closed reflux and colorimetric experimental methods were used. Organic compounds in solid waste eluate, got oxidized completely by potassium dichromate ($K_2Cr_2O_7$) in the presence of sulfuric acid (H_2SO_4) to produce CO_2 and H_2O . 2.5 mL sample was put in COD tubes then 1.5 mL $K_2Cr_2O_7$ and 3.5 mL H_2SO_4 were added. These samples were heated for 2 hours at 150 °C in a COD digester. After digestion, COD was determined colorimetrically against standards using the Hach DR 2800 Spectrophotometer at 600 nm (USA).

4.4.1.3. Total Kjeldahl Nitrogen (TKN) Analysis. Total Kjeldahl Nitrogen (TKN) experiment was conducted according to the specific method of equipment (HACH-Method 8075). HACH Digesdahl Digestion Apparatus, 115 Vac (USA) device was used. Solid waste sample was added to 100 volumetric flask then 4 mL of concentrated sulfuric acid was added. The sample was heated until acid vapor was present in the flask and additional 4 minutes for sulfuric acid to reach boiling point. 50% hydrogen peroxide was added and heated for one minute to allow for complete evaporation of excess hydrogen peroxide. 5 mL of digested sample was measured by using a spectrophotometer.

4.4.1.4. Total Organic Carbon (TOC) Analysis. Total Organic Carbon (TOC) analysis was performed for MSW characterization measurements. TOC measurements were also performed during the leaching test experiments. The leachate samples taken at specific times during high ionic strength experiments were analyzed for total organic carbon before ion chromatography (IC) analysis. This is a required procedure to determine dilution factors before IC analysis for preservation of the IC device, as explained above. Samples were diluted according to conductivity parameters measured during tests for TOC analysis. After dilution step, leachate samples were

filtered with 0.45 μm Syringe Filters. TOC measurements were conducted with a Shimadzu TOC-V Total Organic Carbon Analyzer (Japan) with SM 5310C standard method.

4.4.1.5. Ion Chromatography (IC) Analysis. Ion Chromatography (IC) measurements were performed during MSW characterization. According to TOC analysis results, were conducted based on SM 4110 standard method using a Dionex ICS-3000 Ion Chromatography (Thermo Fisher Scientific, USA) device. In Table 4.3, the limit of detection for IC was shown.

Table 4.3. The limit of detection of ions for Ion Chromatography (IC).

IC	
Parameters	LOD (mg/L)
F	0,005
Cl	0,023
NO ₂	0,005
Br	0,012
NO ₃	0,023
SO ₄	0,013
PO ₄	0,011

4.4.1.6. Microwave Assisted Digestion Method. In order to determine the concentration changes of Zn in leachate from the batch reactors, 5 mL of leachate samples were taken at determined times from each batch reactor during three days. Each sample was digested according to the procedures by Microwave Assisted Digestion Method 3030 K as outlined in Standard Methods (APHA, 1998) by using a MARS 6 Microwave Accelerated Reaction System Instrument (CEM Corporation, USA). After microwave digestion, DI water was added to the resulting solution up to 50 mL. Then Zn concentration in the sample was analyzed with ICP-OES. The measurements were performed as triplicates and the average concentration was recorded. Table 4.4 shows the standard digestion method in detail.

Table 4.4. Digestion method for determination of Zn.

NP	Method	MW Operating Temperature
ZnO	8 mL HNO ₃ + 2 mL H ₂ SO ₄	200 °C

In Table 4.5, microwave parameters are shown for every step in detail.

Table 4.5. Microwave operating parameters.

STAGE	RAMP (min.)	HOLD	TEMPERATURE (°C)	PRESSURE	POWER (W)
1	15	5	140	400	1600
2	16	15	200	400	1600

4.4.1.7. Inductively Coupled Plasma Optical Emission Spectroscopy (ICP-OES) Analysis. In order to determine Zn concentration in leachate samples, an inductively coupled plasma optical emission spectroscopy (ICP-OES) PerkinElmer OES Optima 2100 DV (USA) was used. The leachate samples were pre-treated before ICP-OES analysis in order to determine Zn concentrations. Each sample was filtered using 0.45 µm Syringe Filter before ICP - OES analysis. The measurements of Zn for coated and dispersion ZnO NPs sets were conducted using ICP-OES, for the uncoated ZnO NP sets, Zn was analyzed using an AAS-OES due to a technical problem with ICP-OES during that time. However, several certain samples were also analyzed with PerkinElmer ICP-OES in order to compare the reliability of results and there was no significant difference observed. The limits of detection (LOD) value of ICP-OES are listed in Table 4.6.

Table 4.6. The limit of detection (LOD) of metals for ICP-OES.

ICP-OES	
Parameters	LOD (mg/L)
Al	0.004
Cd	0.001
Co	0.002
Cr	0.005
Cu	0.003
Fe	0.005
Pb	0.004
Mn	0.003
Mo	0.004
Ni	0.004
Zn	0.004
Si	0.008

The Zn analysis was conducted based on TS EN ISO 11885 standard method (TS EN ISO 11885, 2013).

4.4.1.8. Particle size distribution analysis. Selected samples were measured for particle size determination. The samples from 0., 6., 12., 24., 48. and 72. hour of 100 mg/L reactors of coated and uncoated nano ZnO sets were analyzed for particle size distribution. Brookhaven 90 Plus (Nova Instruments, USA) equipment was used for the measurements. The device is aimed to analyze the concentrated suspensions of small particles or solutions of macromolecules. The particle size measurement range is between 2nm to 3 μ m. High concentration reactor samples were selected for particle analysis. Therefore, 100 mg/L reactor samples obtained at certain time intervals were used. Selected samples were put into a tube and then the tube was inserted into the device for measurements.

5. RESULTS AND DISCUSSION

In this section, characterization of solid waste and leaching experiment results will be discussed.

5.1. Initial Solid Waste Analysis

The results of the initial characterization of municipal solid waste (MSW) are given in this part. The background characterization of fresh municipal solid waste that was taken from İZAYDAŞ disposal facility was performed. The initial characterization data is shown in Table 5.1.

Table 5.1. Characterization of municipal solid waste.

Parameter	Unit	Sample 1	Sample 2
TS	%	40.79	34.5
MC	%	59.21	65.5
VS	%	27.91	-
COD	mg/L	3038	-
pH	-	5.99	-
Conductivity	mS/cm	4.65	-
TOC	mg/L	2448	-
TKN	mg/L	10.1	-
Cl ⁻	mg/L	494	-
NO ₃ ⁻	mg/L	607	-
SO ₄ ²⁻	mg/L	1495	-
PO ₄ ³⁻	mg/L	94	-
Titanium (Ti)	mg/kg	1423	1158
Silver (Ag)	mg/kg	ND*	8.6
Silicon (Si)	mg/kg	360	160
Zinc (Zn)	mg/kg	239	115
Aluminium (Al)	mg/kg	6332	157
Cadmium (Cd)	mg/kg	0.8	0.3
Cobalt (Co)	mg/kg	8	3.6
Crom (Cr)	mg/kg	48	97.4
Copper (Cu)	mg/kg	103	76.4
Iron (Fe)	mg/kg	15289	108
Mangan (Mn)	mg/kg	208	248
Molibden (Mo)	mg/kg	2.7	2.4
Nickel (Ni)	mg/kg	34	21
Lead (Pb)	mg/kg	907	17.2

*ND: Non-detected

The background characterization analyzes were performed with two different solid waste samples which were taken at different times. They were labeled as Sample 1 and Sample 2. Sample 1 was used to get more comprehensive information regarding the characterization of solid waste in general. It includes total solids (TS), moisture content (MC), volatile solid (VS), COD, pH, conductivity, TOC, TKN, ions (Cl^- , SO_4^- , and NO_3^-) and metal analyses. Sample 2 refers the initial characterization of the solid waste samples that were used for nano ZnO batch reactor tests. TS, MC and metal analyses were done using Sample 2. The COD and TOC measurements were conducted with samples from eluate whereas other measurements conducted using fresh MSW samples.

In Table 5.1., all the results regarding Sample 1 and Sample 2 are shown. Moisture content values of solid waste were 59.21 % and 65.5 % in Sample 1 and 2, respectively. These are average rates for Turkish solid waste characteristics. Zn was detected as 239 mg/L in Sample 1, whereas it was recorded as 1155 mg/L in Sample 2. Former value was about half of the first one. When the metal analyses of each sample were compared, there was a big difference between Fe, Pb, Si and Al results. The results were extremely low in Sample 2. Since MSW is not separated at source, high and/or variable metal concentrations can be observed in Turkish MSW. In addition, as expected, real MSW sample contents may differ with time and season, therefore, the characterization results might be very different from each other.

5.2. Leaching Experiments with ZnO NP

In this experimental research, the leaching potential of nano-ZnO in municipal solid waste was investigated considering different environmental conditions such as acidic and basic pH ranges and high ionic strength using batch reactors. Various types of ZnO NPs were used to determine how the leaching potential was affected by the properties of the nanoparticles. The experiments were performed with uncoated (powder), powder Z-Cote HP1 (coated) and dispersion (slurry) ZnO NPs. Table 5.2 shows the properties of each experimental set. In total, 9 sets of experiments were conducted to evaluate the leaching behavior of nano ZnO from fresh municipal solid waste.

In order to adjust acidic, basic and high ionic strength conditions in batch reactors, required adjustments for each kind of conditions were done as mentioned before in Material and Methods section in detail.

The initial pH range for acidic reactors was about 7, and it was about 12 for the basic reactors. The pH of solid waste tended to be close to the acidic range, due to rapid decomposition of the

organic fraction of the MSW. Therefore, 1-2 mL of 6 N H₂SO₄ was enough to adjust the required range. In order to adjust basic condition in the system, 15-20 mL of 1 N NaOH was initially added to each batch reactor. For high ionic strength experiments, 0.6 mg NaCl was initially added to the reactors.

The complete results including pH and conductivity and the Zn concentration values from Set 1 to Set 9 are shown in Appendix.

Table 5.2. Properties of each experimental set.

SET	ZnO Type	pH	High Ionic Strength	Added ZnO Concentration (mg/L)
1	Uncoated	Acidic	Unadjusted	0, 10, 25, 100
2	Uncoated	Basic	Unadjusted	0, 10, 25, 100
3	Uncoated	Unadjusted	Adjusted	0, 10, 25, 100
4	Powder Z-Cote HP1	Acidic	Unadjusted	0, 10, 25, 100
5	Powder Z-Cote HP1	Basic	Unadjusted	0, 10, 25, 100
6	Powder Z-Cote HP1	Unadjusted	Adjusted	0, 10, 25, 100
7	Dispersion	Acidic	Unadjusted	0, 10, 25, 100
8	Dispersion	Basic	Unadjusted	0, 10, 25, 100
9	Dispersion	Unadjusted	Adjusted	0, 10, 25, 100

5.2.1. Leaching Experiments with Uncoated ZnO NPs

In this experimental set, uncoated ZnO NP that was purchased from Sigma Aldrich was used. The batch reactors contained 0 (control reactor), 10, 25 and 100 mg/L concentrations of ZnO NP, respectively. Set 1, 2 and 3 refer to the uncoated ZnO NP experiments as acidic, basic and high ionic strength conditions, respectively.

In uncoated ZnO NP-acidic set experiments (Set 1), in all reactors, the pH range changed between 5 and 6 with time as shown in Figure 5.1. There were no observed notable changes in all reactors.

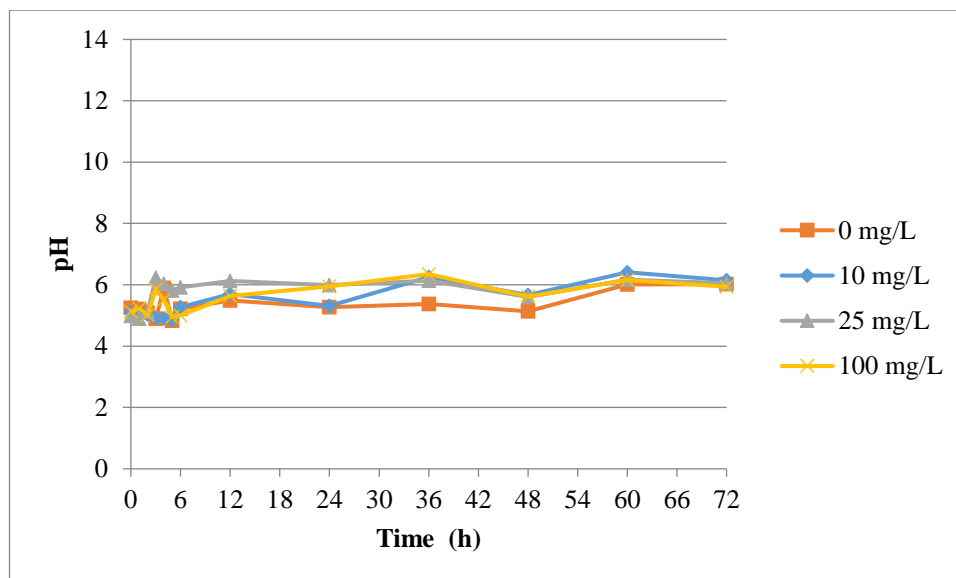


Figure 5.1. The pH change in uncoated ZnO NP-acidic set reactors with time (Set 1).

The Zn concentration in leachate differed in reactors versus time (Figure 5.2). The measured initial Zn concentrations of 0, 10, 25 and 100 mg/L batch reactors were 5.31, 7.44, 18.56 and 46.86 mg/L, respectively. The final concentrations, at the end of 3th day, were 4.36, 2.22, 5.55 and 18.46 mg/L, in 0, 10, 25 and 100 mg/L batch reactors, respectively. In control and 10 mg/L reactors, Zn concentrations were detected at low levels. The concentration in control reactor was about 5 mg/L and did not change much. The concentration of Zn in 10 mg/L reactor decreased with time. The Zn concentration in 100 mg/L reactor decreased during 36 hours and after the 36th hour it was stabilized relatively. The Zn concentration of 25 mg/L reactor also decreased in the first 36 hours and after then represented a constant trend with respect to time.

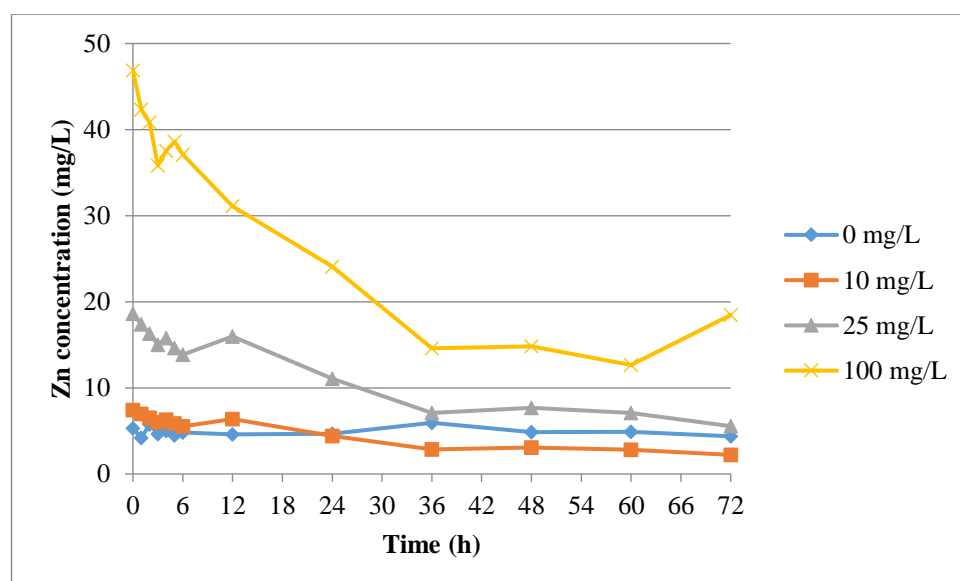


Figure 5.2. The Zn concentration change in uncoated ZnO NP-acidic set reactors with time (Set 1).

In Set 2, the behavior of nano ZnO under basic pH conditions was investigated. The pH change in uncoated-basic reactors was between 12-6 as shown in Figure 5.3. The pH value of the each reactor was higher at the beginning of the experiments, due to initial external pH adjustment, but it decreased dramatically to acidic levels in the 12th hour and after the 12th hour, it showed a constant trend until the end of the experiments. There was no pH adjustment during the experiments.

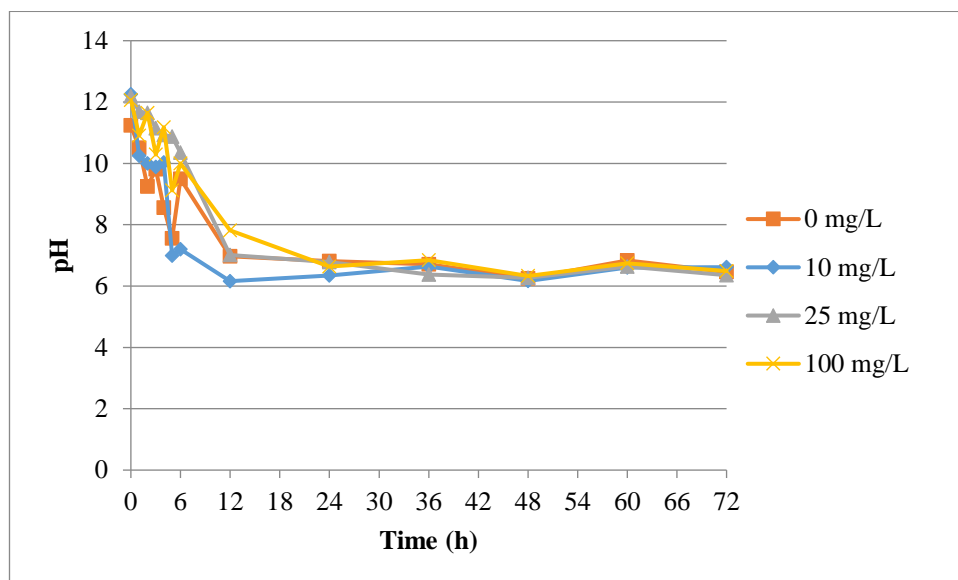


Figure 5.3. The pH change in uncoated ZnO NP- basic set reactors with time (Set 2).

The leaching behavior of Zn also showed a decreasing trend in each reactor versus time (Figure 5.4).

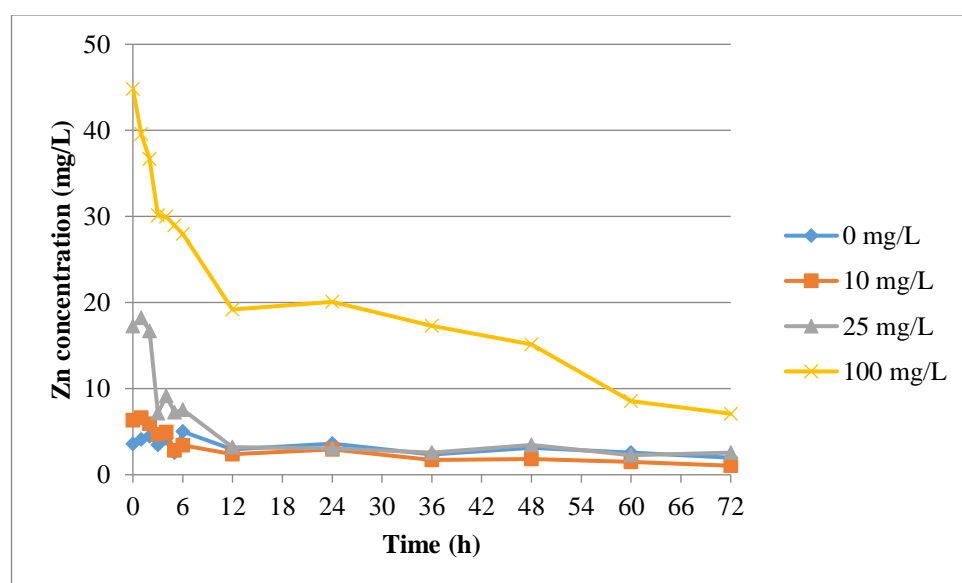


Figure 5.4. The Zn concentration change in uncoated ZnO NP-basic set reactors with time (Set 2).

Initial concentrations in each reactor were 3.59, 6.32, 17.25 and 44.81 mg/L. In addition to this, the final Zn concentrations were also recorded as 1.98, 1.05, 2.56 and 7.08 mg/L, in 0, 10, 25 and 100 mg/L batch reactors, respectively. The Zn concentrations in 10, 25 and 100 mg/L reactors decreased rapidly in the first 6 hours of the experiment. The Zn concentration trend was slightly fluctuating in 10 mg/L reactors after the 6th hour. On the other hand, the Zn concentration in 25 and 100 mg/L reactors decreased more gradually with time.

In uncoated-high ionic strength (set 3) experiments, NaCl was used to obtain high ionic strength conditions and no pH adjustment was done in the reactors as indicated before. The pH values did not change significantly in each reactor and they changed between 5 to 6 (Figure 5.5).

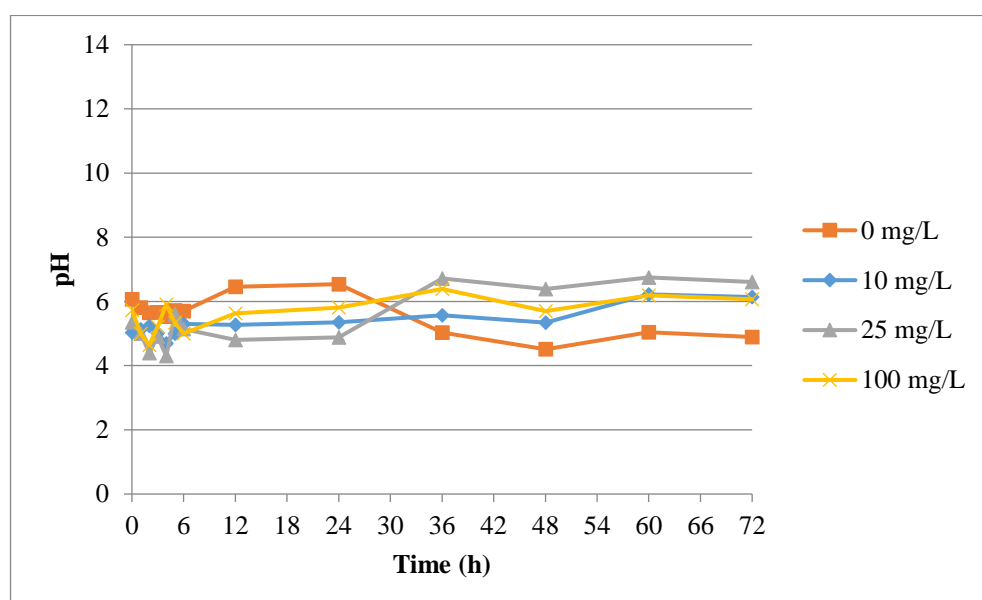


Figure 5.5. The pH change in uncoated ZnO NP-high IS set reactors with time (Set 3).

Figure 5.6 shows the conductivity values of leachate. The conductivity values did not seem to change significantly during the experiments with respect to time.

The Cl⁻ measurements were also performed since high ionic strength reactors were loaded with NaCl in the beginning of the experiments. The Cl⁻ results in 10, 25 and 100 mg/L reactors changed between 900 to 2000 mg/L versus time whereas the Cl⁻ concentration changed between 1100-4500 mg/L in 0 mg/L reactor. The complex matrix of MSW and the difference in the homogeneity between reactors might have caused the significant differences in results.

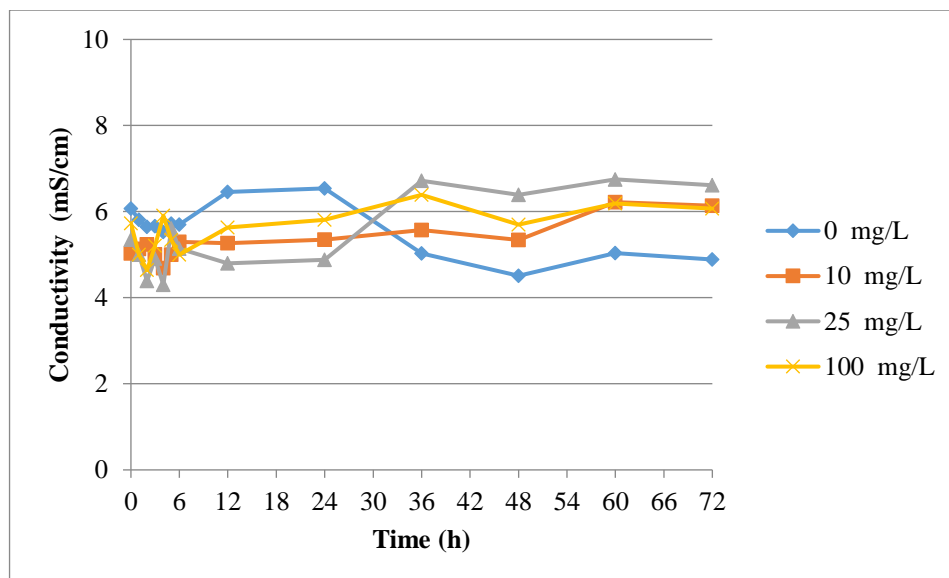


Figure 5.6. The conductivity change in uncoated ZnO NP-high IS set reactors with time (Set 3).

The Zn concentration in leachate decreased by time as it was observed in uncoated-basic set experiments (Figure 5.7).

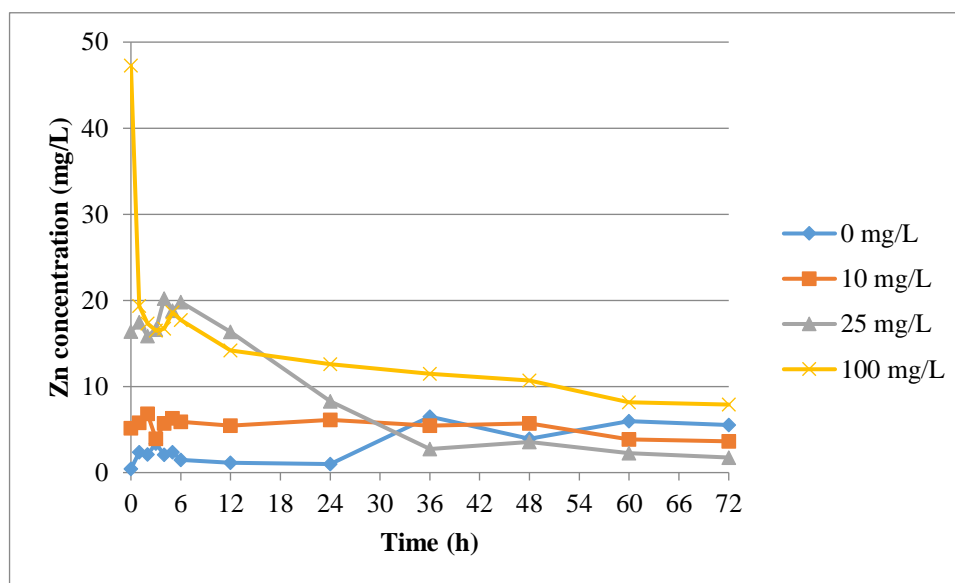


Figure 5.7. The Zn concentration change in uncoated ZnO NP-high IS set reactors with time (Set 3).

Initial recordings were 0.42, 5.16, 16.37 and 47.27 mg/L in 0, 10, 25 and 100 mg/L reactors, respectively. The final concentration values of each reactor were analyzed as 5.54, 3.63, 1.75 and 7.9 mg/L, respectively. Significant decreases were monitored in 25 and 100 mg/L reactors by time. This descending trend was preceded during three days. The Zn concentration in 25 mg/L reactor fluctuated in first six hours but it started to decrease after the 6th hour and reached 1.75 mg/L at the

end of the experiments. In 100 mg/L reactor, the initial concentration was recorded as 47.27 mg/L in the beginning of the experiments but it decreased expeditiously in the first hour and measured as 7.9 mg/L in the end. On the contrary, the Zn concentration change in 10 mg/L reactor did not differ considerably. It fluctuated in the first six hours but continued in close values to initial concentration until 60th hour. In 0 mg/L reactor, there was monitored an unexpectedly increase after 24th hour. The leaching of Zn content from MSW (background Zn content) might have caused this increase in concentration.

When the results obtained in three sets (Set 1-3) of experiments are evaluated as a whole, it can be seen that the particular nano ZnO used tended to stay within the MSW matrix rather than moving with the leachate. Different environmental conditions, such as acidic pH, basic pH and high ionic strength, did not have a considerable effect on the leaching potential of uncoated nano ZnO to the leachate.

When the leaching results of uncoated nano ZnO under three different environmental conditions are discussed, the Zn concentrations in leachate decreased with respect to time and steady-state conditions were attained at the end of 72th hour. Even though the same MSW sample was used for these sets, slight differences in waste composition in each batch reactor might have affected the leachate Zn concentrations during the experiments.

5.2.2. Leaching Experiments with Z-Cote HP1 ZnO NPs

In Z-Cote HP1 ZnO NP experiments, the reactors were loaded with ZnO NP obtained from BASF.

Sets 4, 5 and 6 refer to the Z-Cote HP1 ZnO NP experiments as acidic pH, basic pH and high ionic strength conditions, respectively.

In set 4, the leaching behavior of Z-Cote HP1 ZnO NPs was observed under acidic pH conditions. For the Z-Cote HP1 ZnO NP-acidic set reactors (set 4), the pH change of leachate was almost constant during 72 hours and the pH tended to stay within the acidic range in all reactors during the entire experiment (Figure 5.8).

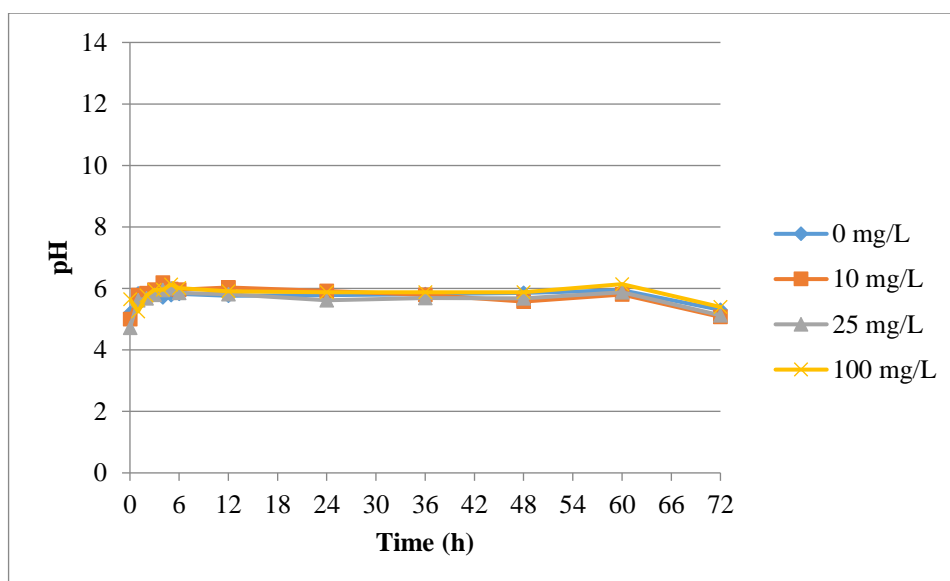


Figure 5.8. The pH change in Z-Cote HP1 ZnO NP-acidic set reactors with time (Set 4).

The initial Zn concentrations were measured as 4.03, 2.72, 3.01 and 13.45 mg/L in 0, 10, 25 and 100 mg/L reactors, respectively.

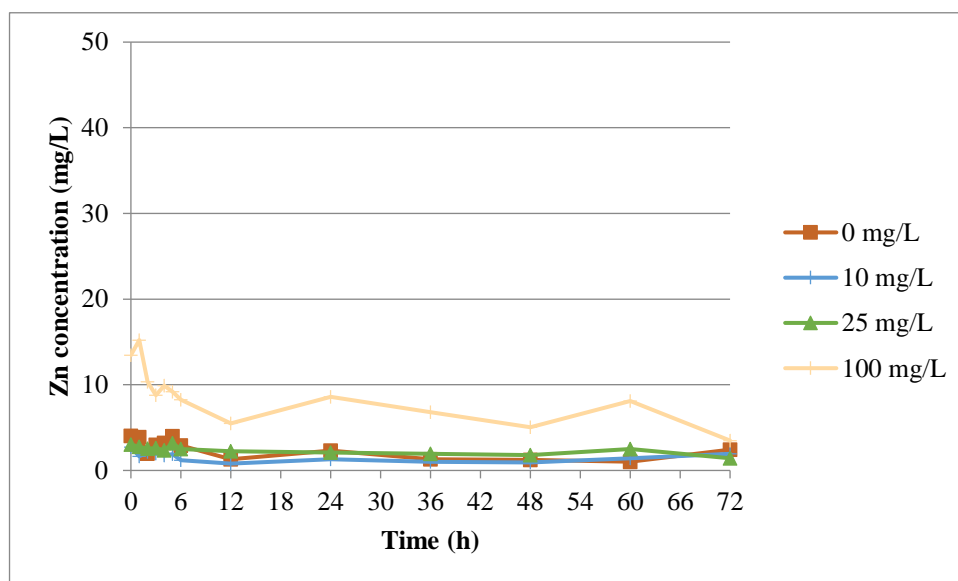


Figure 5.9. The Zn concentration change in coated ZnO NP-acidic set reactors with time (Set 4).

The concentration values demonstrated a descending tendency throughout the experiments in all reactors. Particularly, the concentrations of 10 and 25 mg/L reactors were extremely at low levels with exception of the fluctuations in the first six hours. However, the Zn concentration of 100 mg/L reactor showed a decreasing tendency although it slightly fluctuated at 24th and 60th hours (Figure 5.9).

In Z-Cote HP1 ZnO NP-basic set experiments (set 5), the initial pH value was adjusted to above basic levels, to about 12, using NaOH stock solution, as stated before. After experiments were started, the pH value decreased gradually until the end of tests and reached about 6-8 (Figure 5.10).

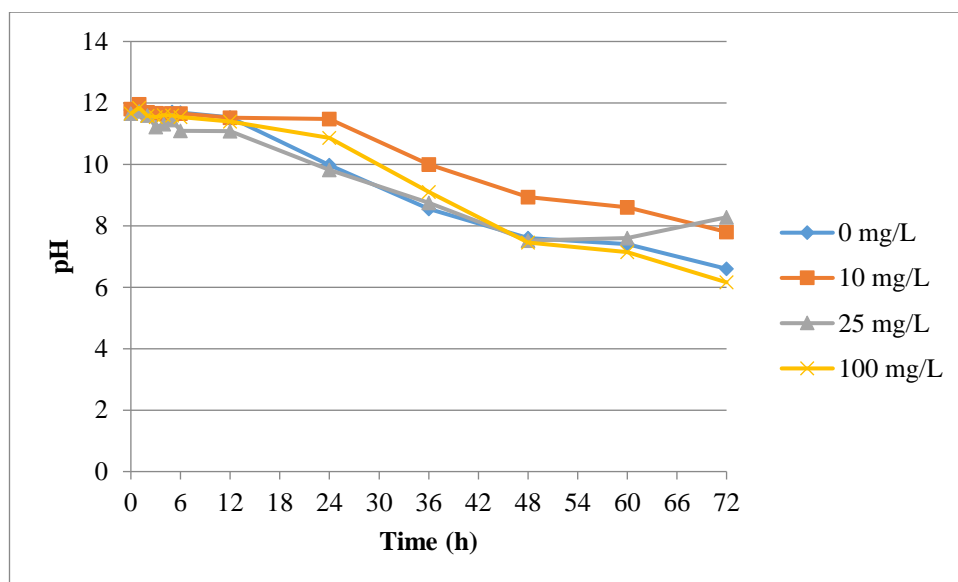


Figure 5.10. The pH change in Z-Cote HP1 ZnO NP-basic set reactors with time (Set 5).

This notable decrease in basic set reactors pH values was due to rapid acidification of the organic fraction of the MSW. Since the buffering capacity of the system was not adequate to buffer this pH decrease, the pH decreased gradually versus time, however, towards to the end, the pH decrease relatively stabilized.

The leaching behavior of Z-Cote HP1 nano ZnO under basic conditions demonstrated similar trends with the acidic condition results (set 4). Initial Zn concentrations were recorded as 1.9, 9.18, 7.53 and 30 mg/L in 0, 10, 25 and 100 mg/L reactors, respectively. The leachate Zn concentration levels of 10 and 25 mg/L reactors were at low levels; however, the concentration of 100 mg/L reactor decreased with time substantially as shown in Figure 5.11. During the experiments, Zn concentration in 100 mg/L reactor showed a dramatic decrease in the first six hours of the experiment. The measured Zn concentration values in 0, 10 and 25 mg/L were at low levels compared to 100 mg/L reactor results. These three reactors showed more stable changes after the 6th hour regarding to leachate Zn concentration.

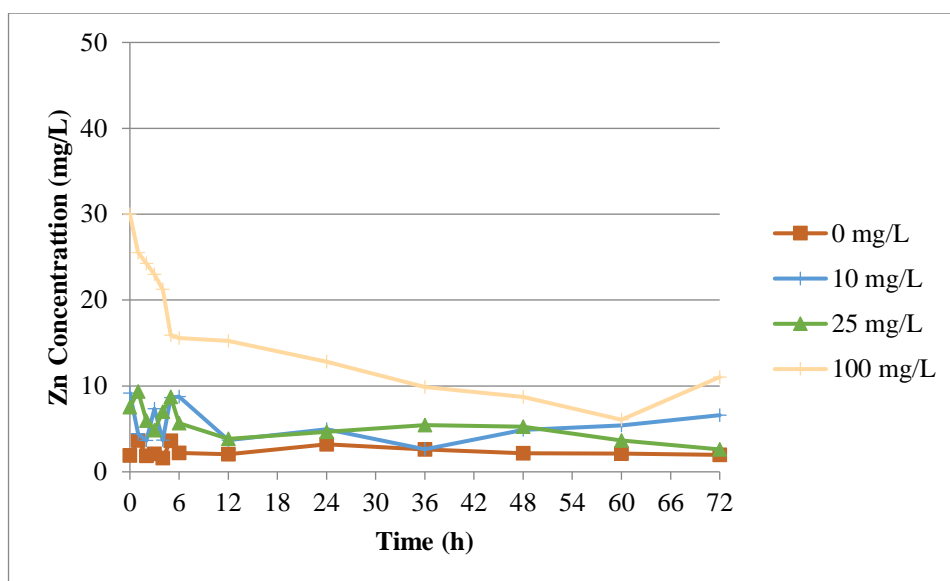


Figure 5.11. The Zn concentration change in Z-Cote HP1 ZnO NP-basic set reactors with time (Set 5).

The leaching behavior of Z-Cote HP1 nano ZnO in high ionic strength test was examined in Set 6.

The pH changes in leachate of reactors for the high ionic strength-adjusted experiments are represented in Figure 5.12. In the beginning of the tests, the pH was about a neutral range but then it dropped to acidic levels by time. It was supposed that decrease in pH was because of the degradation of organic content in municipal solid waste. There was no initial pH adjustment in reactors in this set.

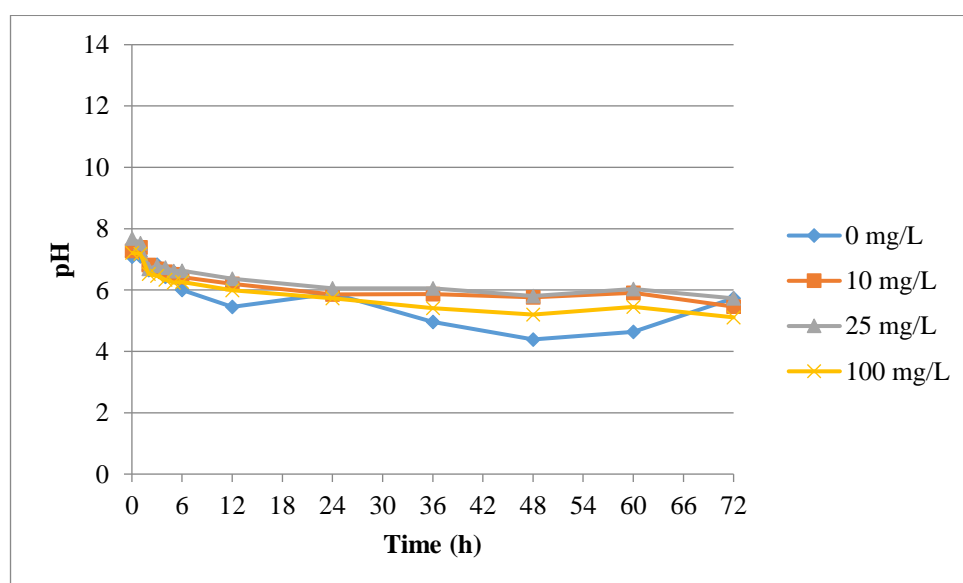


Figure 5.12. The pH change in Z-Cote HP1 ZnO NP-high IS set reactors with time (Set 6).

The Zn concentration results are demonstrated in Figure 5.13 below. Initial Zn concentrations were measured as 0.72, 1.00, 7.02 and 15.88 mg/L in 0, 10, 25 and 100 mg/L reactors, respectively. It was obviously seen that the initial concentrations of each reactor were at low values, even in 100 mg/L reactor, which had the highest Zn concentration reactor. However, the Zn concentrations at the 72nd Hour, which was the last recorded time, were measured as 0.82, 0.84, 4.73 and 9.14 mg/L in 0, 10, 25 and 100 mg/L reactors, respectively. In 100 mg/L reactor, the Zn concentration slightly fluctuated at the 2nd hour, but then it started to decrease during the experiments with respect to time in spite of slight fluctuations.

Regarding the concentration distribution in the 25 mg/L reactor, it was observed that the measured values fluctuated in the first six hours. After the 6th hour, more considerable decrease was observed. On the other hand, the Zn concentration of leachate from 0 and 10 mg/L reactors were at very low levels throughout the experiment and also, they were more stable.

The mobility of ENMs in landfill and landfill leachate depends on the properties of nanoparticles and composition of leachate and waste characteristics as well. However, the release of ENMs changes whether the nanoparticle has coating surfaces or dispersed in bulk (Part et al., 2018). The concentration differences in uncoated, Z-Cote HP 1 and dispersion ZnO NP reactors can partially be explained regarding this information.

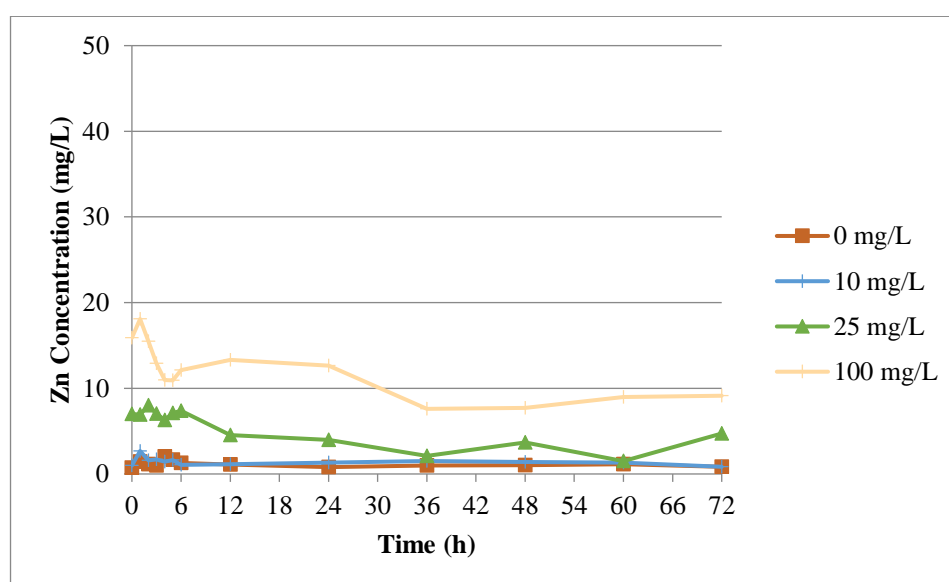


Figure 5.13. The Zn concentration change in Z-Cote HP1 ZnO NP-high IS set reactors with time (Set 6).

In the meantime, the conductivity values of leachate increased with respect to time along the leaching tests as shown in Figure 5.14. In addition to NaCl addition to the reactors, the organic degradation of solid waste by time might cause this increase in conductivity values. The ions release from MSW during the experiment might be the source of this increase. The Cl^- analysis results at leachate differed between 1400-2400 mg/L.

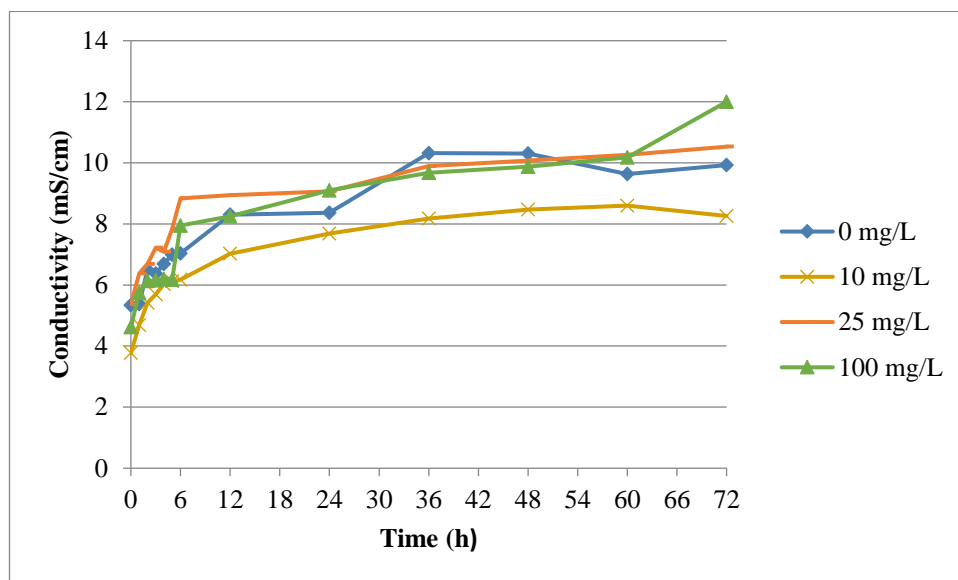


Figure 5.14. The conductivity change in Z-Cote HP1 ZnO NP-high IS set reactors with time (Set 6).

5.2.3. Leaching Experiments with Dispersion ZnO NPs

In these experimental tests, dispersion ZnO NP that was commercially purchased from Sigma Aldrich, was used for preparation of stock solution. Set 7, 8 and 9 indicate related dispersion nano ZnO experiments.

In this experimental test (set 7), the leaching behavior of dispersion ZnO NP was investigated in an acidic pH environment. In acidic condition leaching tests (set 7), the pH value did not change much like in other acidic condition sets (Figure 5.15). The leachate pH values of all reactors exhibited a similar trend and they all lied within the acidic pH range throughout the experiment. The pH values differed approximately between 4.5 to 6.8 for all the reactors during the experiments.

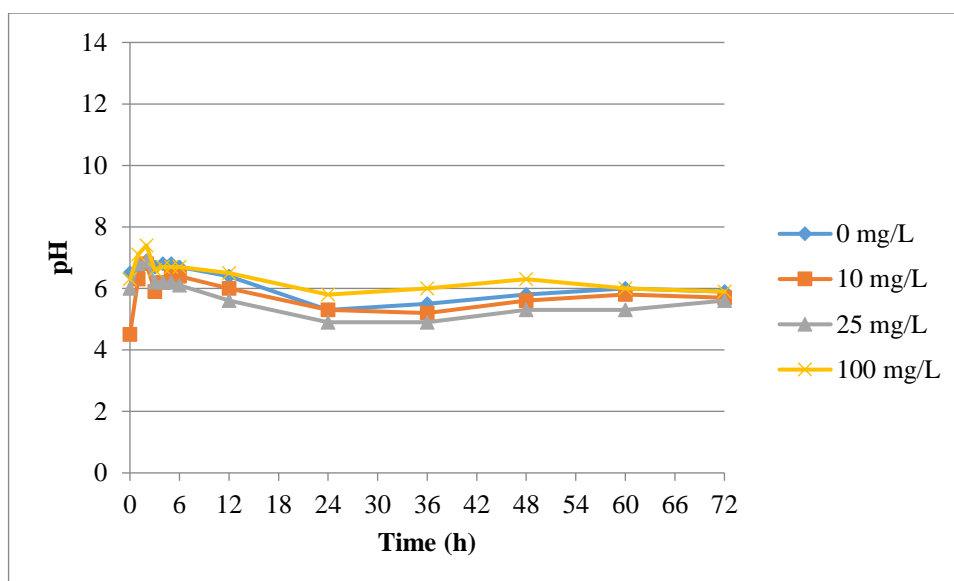


Figure 5.15. The pH change in dispersion ZnO NP-acidic set reactors with time (Set 7).

Figure 5.16 shows leachate Zn concentrations for the dispersion ZnO NP acidic pH set.

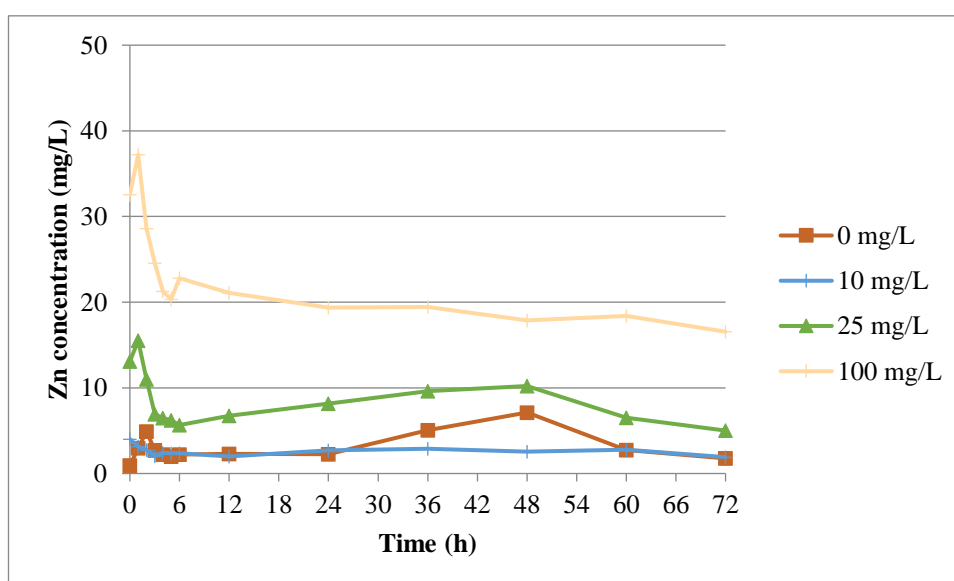


Figure 5.16. The Zn concentration change in dispersion ZnO NP-acidic set reactors with time (Set 7).

The initial Zn concentrations were 0.93, 4.01, 13.09 and 32.54 mg/L and the final measurements at the end of the third day were recorded as 1.78, 1.91, 5.01 and 16.55 mg/L in 0, 10, 25 and 100 mg/L reactors, respectively. Apart from the slight fluctuations during the first sixth hours, the Zn concentration in 100 mg/L reactor was in a gradual decreasing trend. On the other hand, the distribution trend of Zn in 0 and 25 mg/L reactors was very similar to each other (Figure 5.16). An increase occurred in Zn concentration of leachate between 24 and 60 hours in 0 mg/L reactor. This might probably have taken place due to the dissolution of Zn^{2+} ions from the MSW

(background MSW Zn content). The Zn concentration in 25 and 100 mg/L reactors were measured at higher levels, whereas 0 and 10 mg/L measurements were in low levels as expected during the study.

In Set 8, the reactors were adjusted to operate under basic pH conditions to observe the leaching behavior of dispersion nano-ZnO. In this experimental set, the pH and concentration change of Zn were observed versus time. For the basic pH condition dispersion nano ZnO tests, the pH values were in the basic range for the first 12 hours, and then they demonstrated a decreasing trend in all reactors. Even the pH reached to acidic levels in 0 and 100 mg/L reactors towards to the end of the study (Figure 5.17). As explained previously, the degradation of organic content in solid waste caused the pH drop in all reactors.

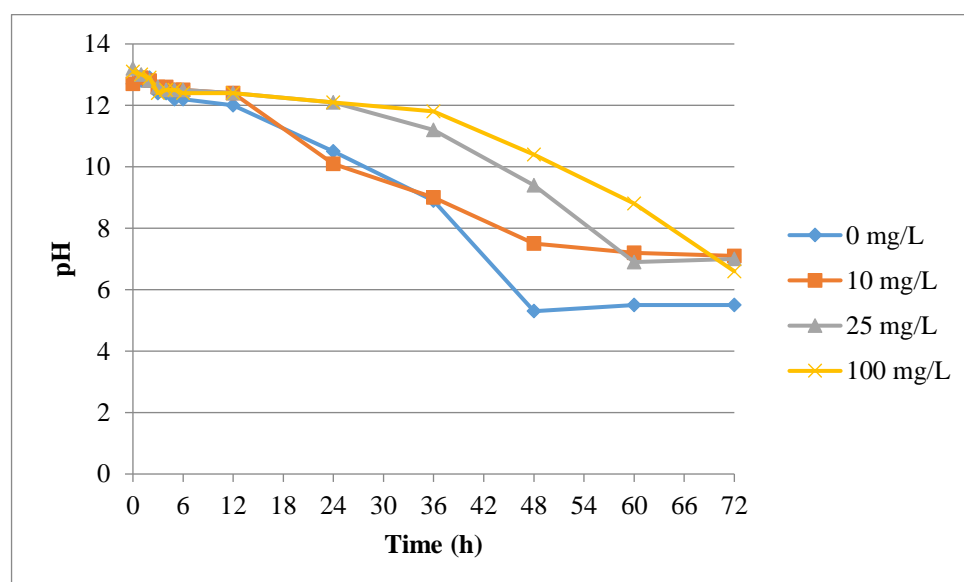


Figure 5.17. The pH change in nano dispersion ZnO NP-basic set reactors with time (Set 8).

The Zn concentrations in basic tests were measured at high levels as seen in Figure 5.18. The initial Zn values were recorded as 0.52, 5.71, 14.19 and 44.35 mg/L in 0, 10, 25 and 100 mg/L reactors, respectively. The final Zn measurements of each reactor were 0.75, 2.54, 5.11 and 19.55 mg/L, respectively. The concentration change in 25 mg/L reactor decreased versus time but it still remained relatively high in the end. Focusing on the behavior of Zn in leachate, it was observed that the Zn concentration remained at high levels, particularly in 25 and 100 mg/L reactors at the end of the experiment. In 10 mg/L reactors, there occurred technical problems in measurements of 3., 4., 5., 6. and 12th hour samples, therefore, they were shown as non-detected (ND) in graph.

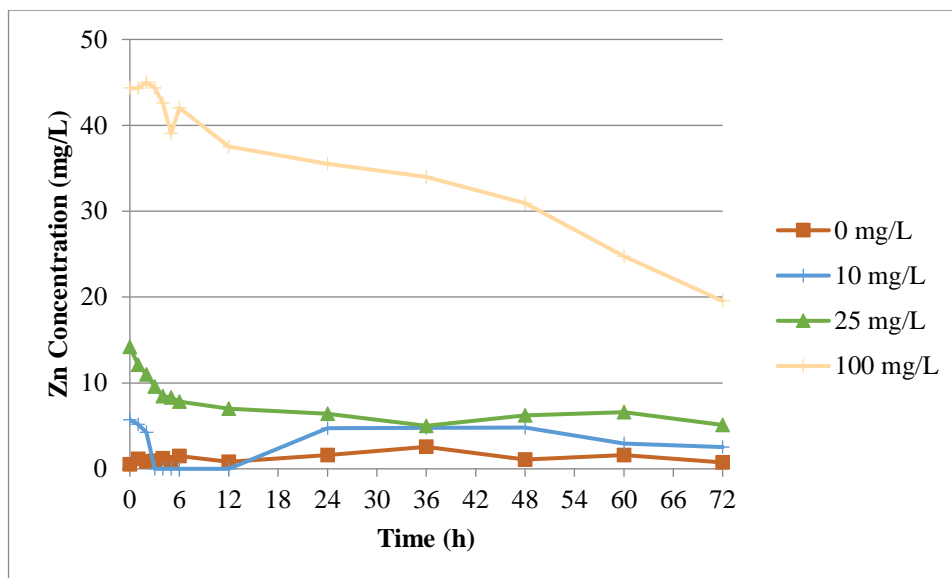


Figure 5.18. The Zn concentration change in dispersion ZnO NP-basic set reactors with time (Set 8).

Set 9 was conducted to investigate the behavior of dispersion nano ZnO under high ionic strength conditions. The pH change in high ionic strength tests is given in Figure 5.19.

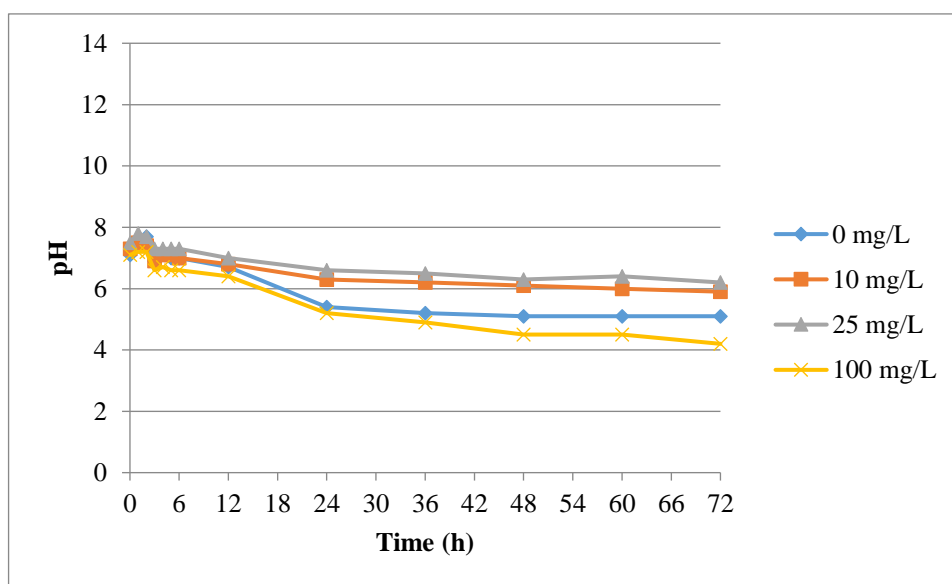


Figure 5.19. The pH change in dispersion ZnO NP-high ionic strength set reactors with time (Set 9).

The initial pH values were in neutral range in all reactors, but later they all started to drop and after 24 hours, they reached acidic levels.

The Zn concentrations in leachate for dispersion-high ionic strength set are shown in Figure 5.20. Likewise, acidic and basic sets, the concentration of Zn in leachate was observed at high levels in high ionic strength sets. The initial concentrations were measured as 0.46, 4.61, 16.77 and 51.6 mg/L, respectively, and the Zn concentrations regarding the 72nd hour values were about 1.74, 2.18, 10 and 22.73 mg/L in 0, 10, 25 and 100 mg/L reactors, respectively. 0 mg/L reactor Zn concentrations were about very low levels. The Zn concentration in 10 mg/L reactor, descended gradually until the sixth hour. After the 6th hour, it increased until the 12th hour and then started to decrease dramatically. The Zn concentration in 10 mg/L reactor started to fluctuate as the experiments started but the values were close to each other. The Zn concentration in 25 mg/L reactor showed a decrease during the first hours. After this point, it started to increase gradually apart from the non-significant fluctuation at 36th hour. In 100 mg/L reactor, Zn concentration values decreased severely until the sixth hour. Then, the Zn concentration did not change significantly in the 100 mg/L reactor until the end of the experiment.

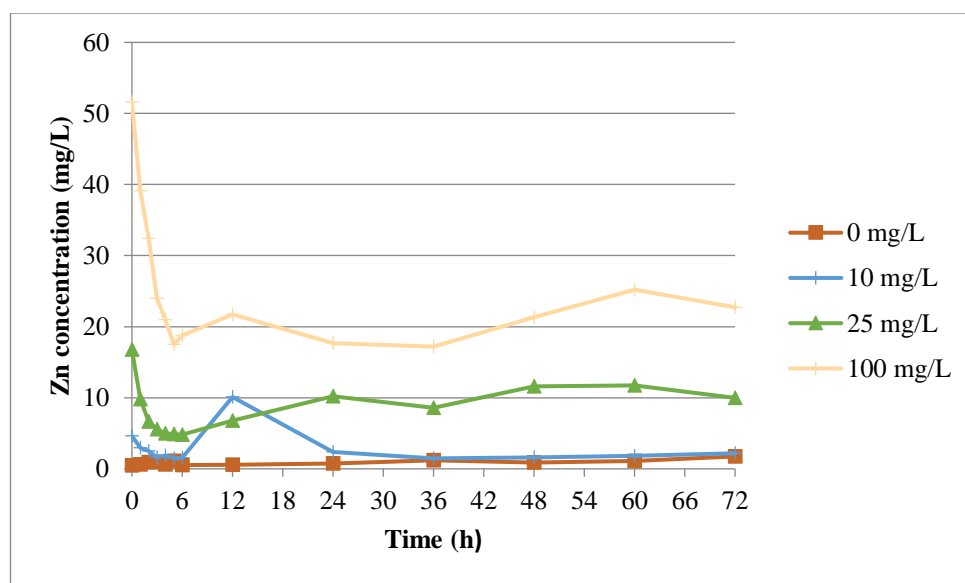


Figure 5.20. The Zn concentration change in dispersion ZnO NP-high ionic strength set reactors with time (Set 9).

Conductivity analysis of leachate for high ionic strength set is displayed in Figure 5.21. The results were within a certain range throughout the experiment in all reactors and did not show any significant change. Regarding the Cl⁻ measurements, the results changed between 640 to 1500 mg/L. The Cl⁻ results of leachate differed in each reactor. This might have been because of the complexity of MSW composition as stated previously.

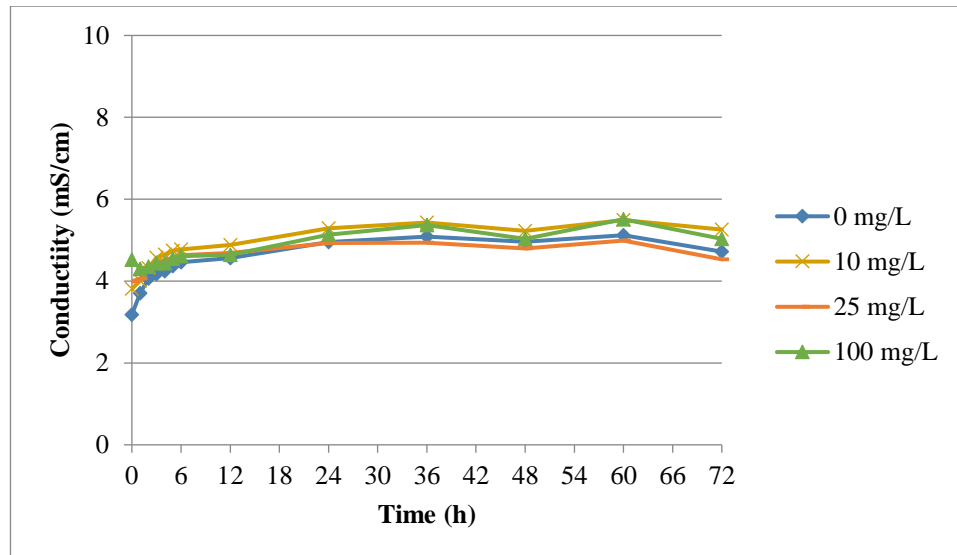


Figure 5.21. The conductivity change in dispersion ZnO NP-high ionic strength set reactors with time (Set 9).

5.3. Comparison of Acidic, Basic and High Ionic Strength Reactors for Each Set

In this research, the leaching behavior of ZnO NPs, using three different featured ZnO NPs (uncoated, Z-Cote HP1 and dispersion), was examined under acidic pH, basic pH and high ionic strength conditions as indicated in Table 5.2. In this section, the leaching behavior of Zn from MSW to leachate for these three different types of ZnO NPs will be discussed and compared with each other.

The total leached Zn mass which was removed from MSW were calculated for each experiment. These calculations were done by using the equation below (5.1).

$$\text{Total Zn mass in leachate} = \sum C_{leached}(t) * V \quad (5.1)$$

The volumes of collected samples were multiplied with each concentration detected with ICP-OES analysis and summed up to determine the total mass of Zn leached from each reactor

The calculated total mass in leachate values for each type of nanoparticles, uncoated, Z-Cote HP1 and dispersion, are demonstrated in Figure 5.22, 5.23 and 5.24 below, respectively.

For the uncoated ZnO NP experiments, the total Zn mass in leachate is shown in Figure 5.22 in detail. As it can be seen, the maximum leached mass was observed in 100 mg/L uncoated acidic pH reactor and the recorded value was 4.71 mg total Zn. Besides, the lowest mass was measured as 0.53 mg under basic condition in 10 mg/L reactor.

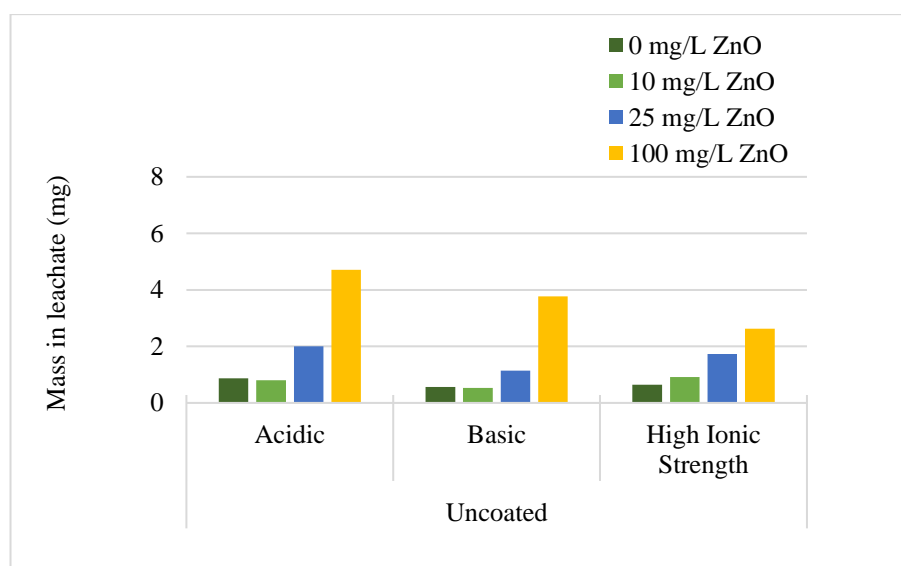


Figure 5.22. Uncoated total (background + any nano Zn added) Zn mass (mg) in leachate.

The maximum leached nano Zn mass for the reactors loaded with coated and dispersion ZnO NPs was observed in 100 mg/L basic set reactors and the measured values were 2.62 and 6.09 mg nano Zn, respectively (Figures 5.23 and 5.24). Similarly, the lowest leaching nano Zn mass values among the lower concentration reactors were detected in 10 mg/L coated ZnO NPs reactor under high ionic strength condition. The results were 0.24 and 0.44 mg nano Zn for reactors containing coated and dispersion nanoparticles, respectively. According to the mass leached results, the highest leaching mass was observed in reactors loaded with dispersion ZnO NPs whereas the lowest values were recorded in coated ZnO NP reactors. The dispersion specification of dispersion nanoparticle could be the reason to be detected in high values than other nanoparticles. However, the surface specification of Z Cote HP1 ZnO NP might have caused to transfer to the liquid part less compared to other nanoparticles. This specific surface property of the nanoparticle might have caused it to stay within MSW matrix mostly. In general, the acidic, basic pH and high IS conditions did not seem to affect the leaching behavior of ZnO NPs selected for this work significantly. However, regarding the uncoated, Z Cote HP1 and dispersion ZnO NP reactors under high ionic strength condition, the total Zn mass in leachate were slightly at low levels. This might be attributed to the decrease of zeta potential with high ionic strength levels. According to DLVO theory, the interaction between ZnO NPs becomes repulsive at low ionic strength levels (Bian et al., 2011). As NaCl concentration increases, a compression occurs in electrical double layer (EDL) thickness so,

EDL decreases (Bian et al., 2011; Han et al., 2014). Therefore, as ionic strength increases, the stability of ZnO NP decreases and agglomeration increases (Bian et al., 2011).

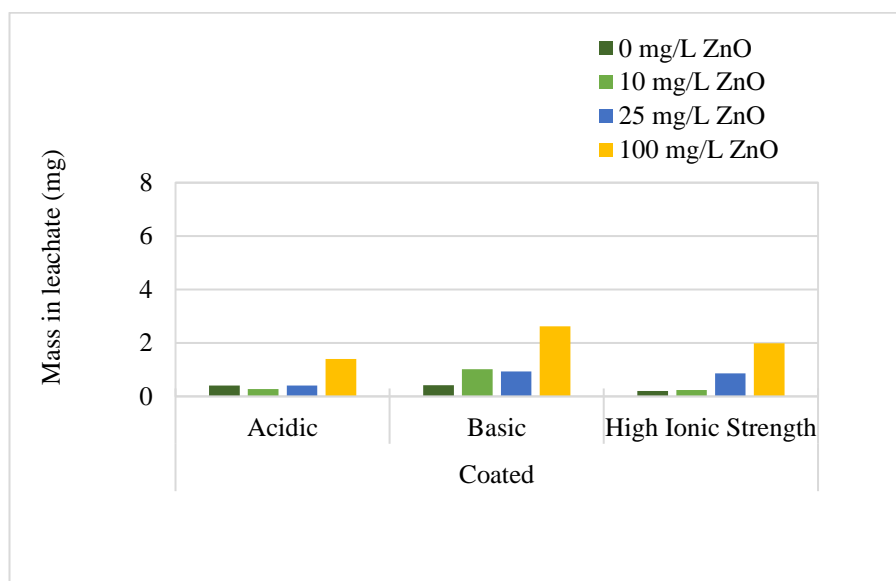


Figure 5.23. Z-Cote HP1 total (background + any nano Zn added) Zn mass (mg) in leachate.

The release of ENMs has been reported to be initiated by physical and chemical conditions such as desorption, diffusion, dissolution and matrix degradation. The attachment/detachment of ENMs and heteroaggregation controls the mobility and transport of nanoparticles. For instance, natural organic matter (NOM) can attach to the surface and prevent the deposition (heteroaggregation) (Part et al., 2018). Since the release is expected to be higher at low pH, any possible heteroaggregation taking place in high pH reactors in our case can be the reason of slightly high total Zn mass in leachate.

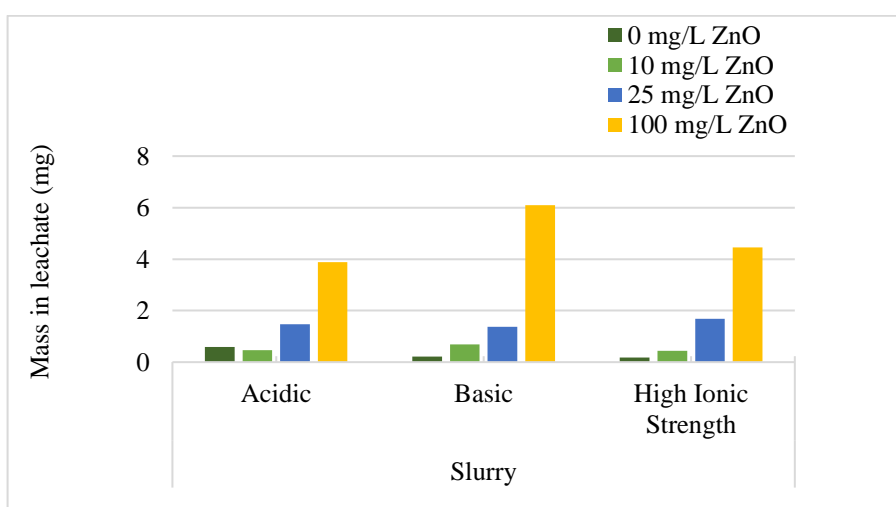


Figure 5.24. Dispersion total (background + any nano Zn added) Zn mass (mg) in leachate.

The mass ratio of Zn in leachate was calculated with the formula in 5.2.

$$\text{Mass \% of nano Zn in leachate} = \frac{\text{Mass Zn leached (mg/L)} - \text{Mass Zn leached from control reactor (mg/L)}}{\text{Mass added (mg/L)}} \times 100 \quad (5.2)$$

The calculated leached mass ratio of uncoated, coated and dispersion nano Zn are given and discussed below.

The leached mass ratios of uncoated nano Zn in acidic, basic and high ionic strength condition are shown in Figure 5.25. The mass in leachate ratios of 0 mg/L reactors were not considered since they were not loaded with ZnO NPs, just were control reactors. The maximum leaching ratio was in 25 mg/L acidic set reactor. There was not observed any uncoated nano Zn leached from MSW to the liquid in 10 mg/L basic and acidic set reactors and about 11.6 % of uncoated nano Zn leached in high ionic strength set reactor. For the reactors containing 25 mg/L ZnO NP, the ratio of uncoated nano Zn mass in leachate was about 0.18 in acidic and high ionic strength sets whereas it was about 0.096, almost the half the others, in basic set. As can be seen, the leached uncoated nano Zn in 100 mg/L reactors was about 16 % in acidic set. The ratios were slightly lower in basic and high ionic strength compared to acidic set ratio. However, the ratio difference between sets was not significant. The uncoated nano Zn in 25 mg/L reactors had the highest mass ratio in leachate among all reactors.

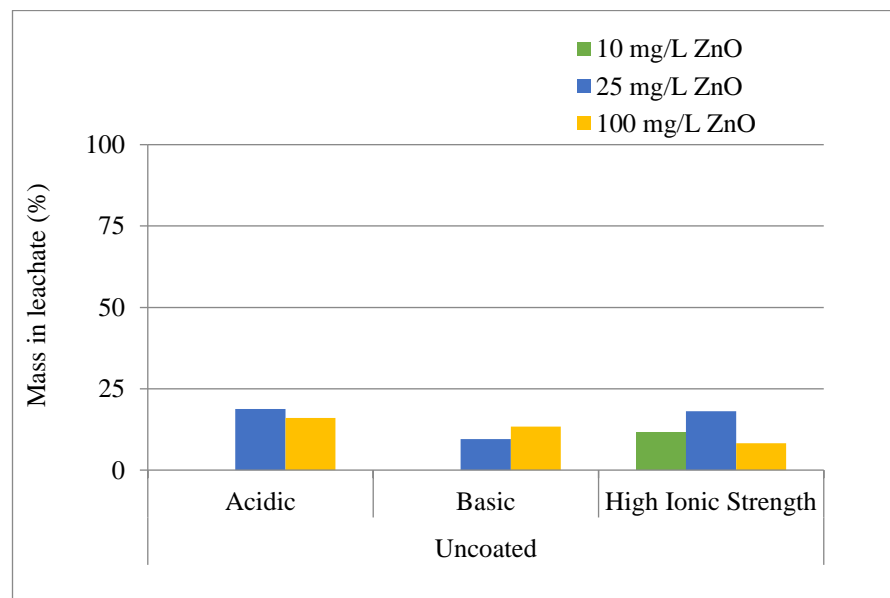


Figure 5.25. Uncoated nano Zn mass in leachate (%).

In Z-Cote HP1 ZnO NPs sets, the maximum leaching, which was about 0.25, was observed in 10 mg/L basic reactor set as shown in Figure 5.26. Under acidic conditions, no Z-Cote HP1 nano Zn leached to the liquid phase in reactors containing 10 mg/L and 25 mg/L Z-Cote HP1 ZnO NP, while only 5% of the nano Zn leached from the reactor with 100 mg/L. Additionally, the lowest and highest ratios are not in a similar trend under acidic, basic and high ionic strength conditions.

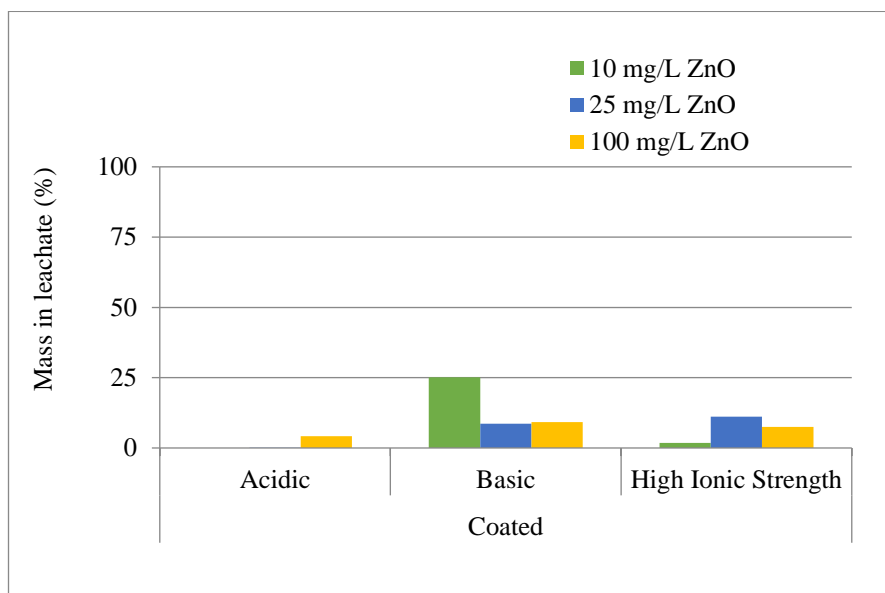


Figure 5.26. Z-Cote HP1 nano Zn mass in leachate (%).

The leaching ratios of dispersion (slurry) nano Zn for three different environment conditions are demonstrated in Figure 5.27. As seen from the graph, mass Zn in leachate ratios, except acidic set reactors, were higher in dispersion ZnO NP reactors compared to other two types of ZnO NP sets. The highest leached dispersion nano Zn ratio among all reactors was in 25 mg/L high ionic strength set reactor as 0.25. The 100 mg/L basic set reactor leached ratio followed it with 0.245, only a very slight difference. Ratios for three different concentrations of reactors were the lowest in acidic set compared with the other two conditions. There was not any leached dispersion nano Zn observed in 10 mg/L acidic set reactor.

For the reactors loaded with uncoated nano ZnO, the maximum leaching ratio was observed in high ionic strength reactors while the maximum leaching ratios were in basic and high ionic strength reactors for Z-Cote HP1 and dispersion nano Zn sets, respectively. However, the maximum ratios were observed in reactors containing 25, 10 and 25 mg/L for uncoated, coated and dispersion sets, respectively.

Dispersion ZnO NP had the highest mass in leachate ratio among the others. This might be the reason of the specification of the nanoparticle as indicated before. The uncoated nano Zn was the second highest one leached to the liquid phase.

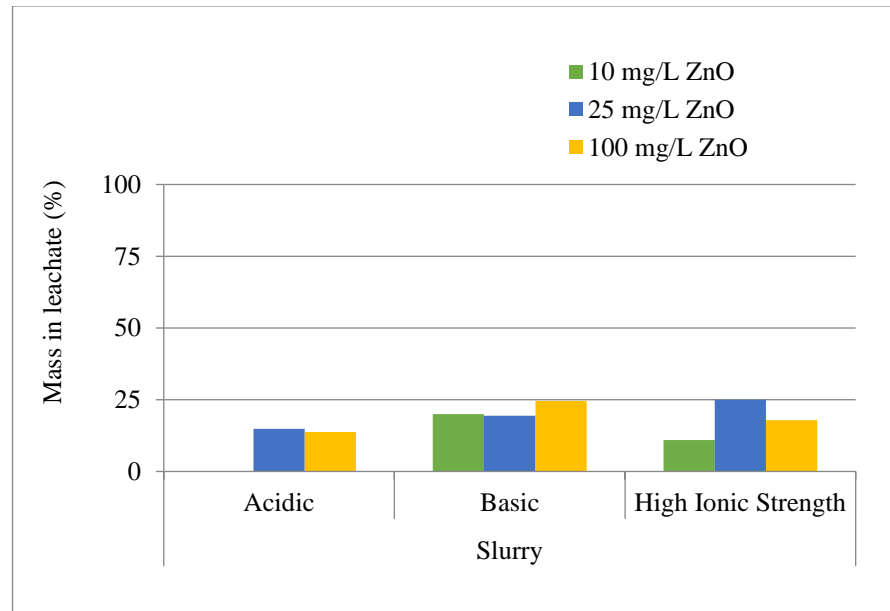


Figure 5.27. Dispersion nano Zn mass in leachate (%).

The retained nano Zn in MSW matrix was also calculated (5.3). The leached nano Zn was subtracted from 100 to find the retained ratio.

$$\text{Mass \% of retained nano Zn in MSW} = 100 - \text{mass of \% Zn in leachate.} \quad (5.3)$$

Figure 5.28, 5.29 and 5.30 show the ratio of retained uncoated, coated and dispersion nano Zn in MSW, respectively.

In uncoated ZnO NP sets, maximum retained ratios in MSW were observed in 10 mg/L acidic and basic reactors with % 100. However, the ratio in 10 mg/L high ionic strength reactor was about 0.88. The ratios for the reactors containing 25 mg/L uncoated nano ZnO stock solution were calculated as 0.81, 0.90 and 0.82 for acidic, basic and high ionic strength condition reactors, respectively. On the other hand, retained Zn ratios were about 0.84, 0.87 and 0.92 in acidic, basic and high ionic strength condition reactors of receiving 100 mg/L nano ZnO stock solution. The average uncoated nano Zn mass retention was calculated about 89.4 % (Figure 5.28).

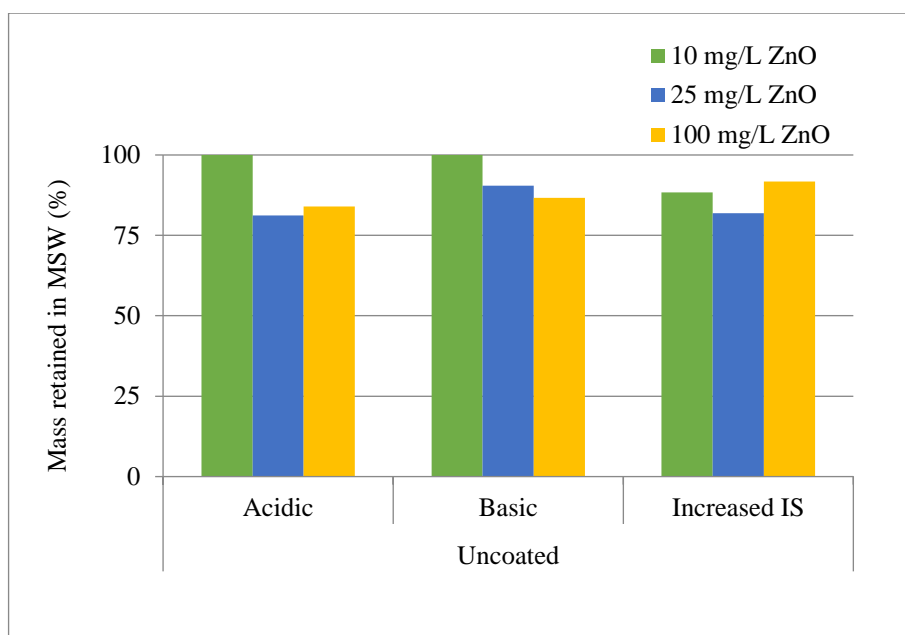


Figure 5.28. Uncoated nano Zn mass retained in MSW (%).

The percentage of coated Zn mass retained in MSW is shown in Figure 5.29 for each set. In acidic sets, reactor receiving 10 mg/L Z-Cote HP1 ZnO NP, nano Zn ratio was retained in MSW entirely. Besides, retained nano Zn mass ratio in 25 mg/L and 100 mg/L reactor were about 99.98 and 95.83 %, respectively. Regarding to basic sets, reactors receiving 10, 25 and 100 mg/L ZnO NP, retained nano Zn in MSW were about 74.9 %, 91.3 % and 90.8 %, respectively. Among them, the lowest mass retained ratio was in 10 mg/L Z-Cote HP1 ZnO basic reactor. In high ionic strength sets the mass retained in MSW were calculated as 98.2 %, 88.9 % and 92.6 % in 10, 25 and 100 mg/L coated ZnO reactors, respectively. The ratios in high ionic strength reactors were also quite high like in other set reactors containing coated ZnO NP. Also, the maximum retained ratios were high in Z-Cote HP1 ZnO NP reactors. The average coated nano Zn mass retention was calculated about 92.5 %. The Z-Cote HP1 nano Zn tended to attach to MSW, most probably due to its surface specification of coated ZnO NP.

The aggregation of ZnO NPs could be influenced by their basic properties (Peng et al., 2015). The attachment efficiency of nanoparticles was reported to decrease with surface coatings (Joo and Zhao et al., 2017). In the light of this information, it can be inferred that the differences of mass retain in MSW percentages of uncoated and Z Cote HP 1 ZnO NPs could be due to their different properties of. Peng et al. also stated that higher levels of electrolytes or higher valent-counter ions might enhance the aggregation in water matrix. The electrolytes or valent-counter ions were not considered in this study (Peng et al., 2015). Since the leachate and MSW might contain these components, this might have also contributed to the aggregation of ZnO NPs.

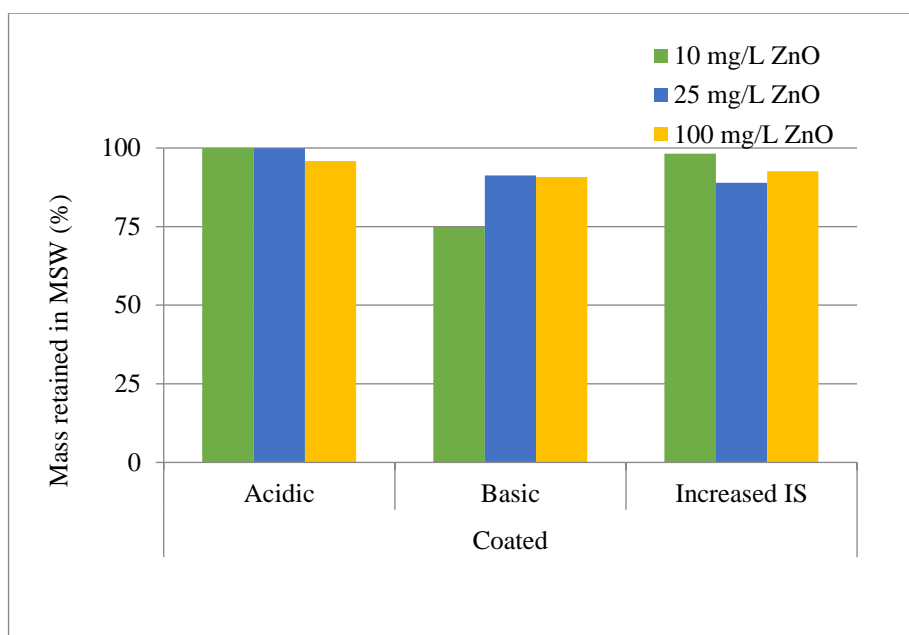


Figure 5.29. Z-Cote HP1 nano Zn mass retained in MSW (%).

Dispersion (slurry) nano Zn behavior is demonstrated in Figure 5.30. In acidic sets, the nano Zn mass retained with 100 % in reactor containing 10 mg/L. However, the dispersion nano Zn mass retained ratios were very close to each other in other reactors. The nano Zn mass retained in MSW were calculated as 85.2 % and 86.3 % in 25 and 100 mg/L reactors, respectively. Based on the results in Figure 5.30, dispersion nano Zn tended to stay in MSW under acidic conditions mostly. In basic sets, the nano Zn mass retained in MSW were close to each other in 10 and 25 mg/L reactors and the values were about 80 % and 80.6 %, respectively. On the other hand, the nano Zn mass retained in MSW in reactor receiving 100 mg/L dispersion ZnO NP was about 75.5 %. In high ionic strength sets, nano Zn mass retained in MSW were calculated as 89.1 %, 75 % and 82.2 % in 10, 25 and 100 mg/L reactors, respectively. Dispersion set Zn mass retention ratios were the lowest when compared to those of both uncoated and Z-Cote HP1 ZnO NP sets. The average dispersion nano Zn mass retention was calculated about 83.8 %. This might have taken place because of the nano ZnO stock solution prepared with dispersion nanoparticle dispersed through the liquid phase more than powder nano ZnO.

The maximum retain ratio was in lower concentration reactors. The pH and IS did not have a significant effect on the ratio of nano Zn mass leached to the aqueous part or retained in MSW. Furthermore, it should also be taken into account that the complex MSW matrix continuously changes as the waste decomposes/stabilizes, affecting the behavior of nano ZnO within the MSW/leachate matrix as well.

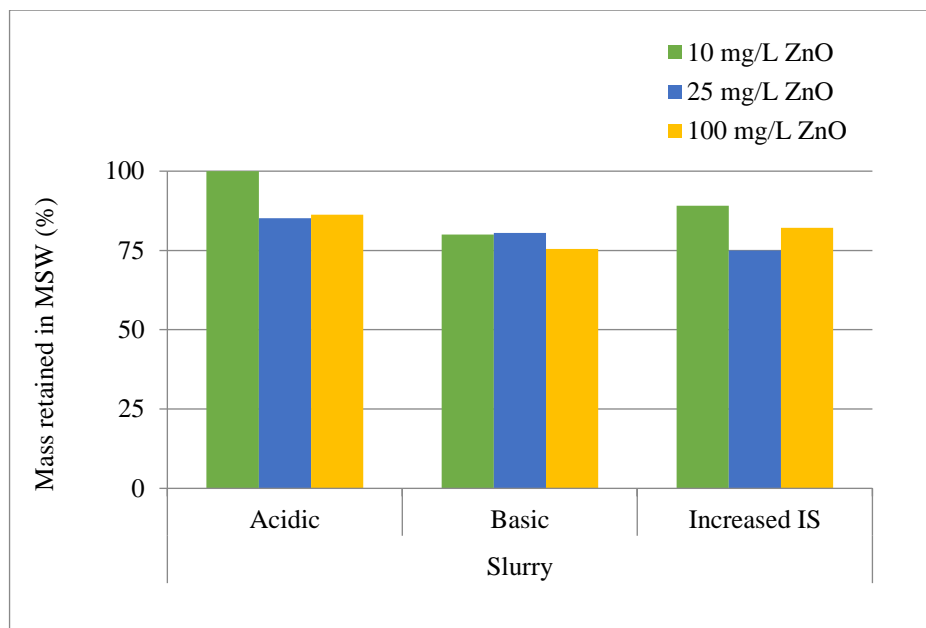


Figure 5.30. Dispersion nano Zn mass retained in MSW (%).

Bian et al. studied the behavior of ZnO NPs in an aqueous matrix. The aggregation behavior of ZnO NPs was influenced by ionic strength, pH and adsorption of humic acid in aqueous solution in accordance with DLVO theory. The release of Zn ions may occur both at low and high levels of pH and increase under certain humic acid concentrations (Bian et al., 2011). However, this research focused only on the behavior of ZnO NPs in leachate-MSW matrix, which is actually a more complex matrix than aqueous solution. In addition, the influence of humic acid, zeta potential and organic content were not considered within this study. It should also be taken into account that the waste stabilization continues and the leachate characteristics change over time as well (Part et al., 2018). Therefore, the Zn concentration under acidic conditions might be slightly at lower levels in this work with respect to expected values from literature.

5.4. Particle Size Distribution Analysis

In this section, the particle size distribution analysis results are discussed. Certain samples were analyzed as mentioned before (0., 6., 12., 24., 48. and 72. hour samples from 100 mg/L reactors). Since 100 mg/L reactors contained the highest concentration of ZnO NP, they were selected for particle size distribution analysis. Particle size measurement of uncoated ZnO samples varied between 402-665 nm for the acidic pH sets, 349-622 nm for the basic sets and 468-857 nm for high ionic strength sets, respectively. In addition, for the coated ZnO sample analysis, the particle size changed between 512-751 nm for acidic pH sets, 376-524 nm for the basic pH sets and 630-763 nm for high ionic strength sets, respectively. Particle size measurement was not conducted for the dispersion nano ZnO tests.

When particle size measurements for powder (uncoated and Z-Cote HP1) ZnO NPs were evaluated, it was generally seen that the particle sizes measured in leachates were greater than those of the size of uncoated and coated ZnO NPs (<100 nm) that were added to the batch reactors. In all measurements, the minimum particle size was greater than 100 nm, showing that the particles formed in the reactor are larger, indicating that the nano ZnO added agglomerated in all cases. In addition, it was observed that the higher IS conditions promoted formation of larger particles in leachate than those for acidic and basic pH conditions for the nano ZnO considered in this work. These results are actually in agreement with the Derjaguin-Landau-Verwey-Overbeek (DLVO) theory that takes into account high particle agglomeration under elevated IS conditions such as leachate-MSW matrix.

6. CONCLUSIONS

In this study, ZnO NP was selected due to the widespread use of it in commercial products. The leaching behavior of different concentrations of uncoated (powder), Z-Cote HP1 (coated) and dispersion (slurry) ZnO NPs from real municipal solid waste samples was observed under different environmental conditions such as acidic pH, basic pH and high ionic strength in batch reactors. The experiments were conducted using 10, 25, 100 mg/L ZnO NPs concentrations and control reactors for 3 days. Based on the results obtained, uncoated and Z-Cote HP1 ZnO NPs tended to remain at waste and a slight portion of uncoated and Z-Cote HP1 ZnO NPs transported to leachate. Dispersion ZnO NPs showed a higher leaching potential among others. However, the maximum mass in MSW ratio was observed in coated ZnO NPs reactors with ratio ranging between 74.86 - 100 %. There was not observed a significant influence of pH on the leaching potential.

In general, the following conclusions can be drawn from this study;

The pH change and conductivity did not seem to affect the released concentration of Zn from MSW significantly. Therefore, the environmental conditions did not affect the leaching behavior of Zn in this study.

In uncoated reactors, the Zn concentrations tended to decrease rapidly in the first hours, followed by a more gradual decrease by time in all sets. A large proportion of ZnO NPs retained in MSW with a large portion.

In Z-Cote HP1 reactors, the Zn concentrations showed a similar trend to the uncoated reactors. Coated ZnO NPs mostly remained in MSW compared to other kind of nanoparticles.

The Zn concentrations trend of dispersion NPs were also in a similar trend with coated and uncoated Zn concentrations. Dispersion ZnO NPs had the highest leaching ratio than those of uncoated and coated ZnO NPs employed in this experimental work. This might be because of the surface stabilization of dispersion ZnO NPs.

There was not a remarkable difference observed in leaching Zn concentrations between uncoated and Z-Cote HP1 ZnO NPs.

Particle size analyses revealed the agglomeration of ZnO NPs in leachate.

Generally, nano ZnO tended to stay within the MSW matrix rather than moving with the leachate for the ZnO NPs selected for this study.

Approximately the retain percentages of ZnO NPs in MSW are 89.4, 92.8 and 83.8 for uncoated, Z-Cote HP1 and dispersion ZnO NPs reactors, respectively.

7. RECOMMENDATIONS

In this research, short term behavior of ZnO NPs was studied. In order to understand and figure out the behavior and leaching of ZnO NPs from municipal solid waste in the long term, simulated landfill experiments are required.

Due to complex matrix of the MSW, the environmental conditions continually change as the waste stabilizes. Thus, the biochemical mechanisms having influence on the long term retention of ZnO NPs should be considered in more detail for further studies.

There is also need to consider heterogeneity, influence of organic matter, and anions and cations contents to obtain more reliable and dependable results.

REFERENCES

APHA/AWWA/WPCF, 1998. Standard methods for the examination of water and wastewater. 20th ed. Washington, DC: American Public Health Association/American Water Works Association/Water Pollution Control Federation, U.S.A.

Allianz-OECD Report, 2016. Opportunities and Risks of Nanotechnologies, Germany-France.

Adeleye A.S., Conway J.R., Garner K., Huang Y., Su Y., Keller A.A., 2016. Engineered nanomaterials for water treatment and remediation: Costs, benefits, and applicability. *Chemical Engineering Journal*, 286, 640–662.

Bashir, S., Liu, J., 2015. *Advanced Nanomaterials and their Applications in Renewable Energy*, Elsevier, U.S.A.

Batley G.E., Kirby J.K., McLaughlin M.J., 2013. Fate and Risks of Nanomaterials in Aquatic and Terrestrial Environments, *Accounts of Chemical Research*, 46-3, 854–862.

Bethi B., Sonawanea S.H., Bhanvaseb B.A., Gumfekar S.P., 2016. Nanomaterials-based advanced oxidation processes for wastewater treatment: A review. *Chemical Engineering and Processing*, 109, 178–189.

Bian S.W., Mudunkotuwa I.A., Rupasinghe T., Grassian V.H., 2011. Aggregation and Dissolution of 4 nm ZnO Nanoparticles in Aqueous Environments: Influence of pH, Ionic Strength, Size, and Adsorption of Humic Acid. *Langmuir*, 27, 6059–6068.

Boldrin A., Hansen S.F., Baun A., Hartmann N.I.B., Astrup T.F., 2014. Environmental exposure assessment framework for nanoparticles in solid waste. *Journal of Nanoparticle Research*, 16, 2394.

Bolyard S., Reinhart D., Santra S., Basumallick S., 2011. Fate of coated zinc oxide nanoparticles in municipal solid waste landfills. 13. *International Waste Management and Landfill Symposium*, Sardinia, Italy.

Bolyard S.C., Reinhart D., Santra S., 2013. Behavior of engineered nanoparticles in landfill leachate. *Environmental Science Technology*, 47, 8114-8122.

Boverhof D.R., Bramante C.M., Butala J.H., Clancy S.F., Lafranconi M., West J., Gordon S.C., 2015. Comparative assessment of nanomaterial definitions and safety evaluation considerations, *Regulatory Toxicology and Pharmacology*, 73, 137-150.

Brar, S.K., Verma, M., Tyagi, R.D., Surampalli, R.Y., 2010. Engineered nanoparticles in waste water and waste water sludge – Evidence and impacts, *Waste Management* 30, 504–520.

Caballero-Guzman A., Sun T., Nowack B., 2015. Flows of engineered nanomaterials through the recycling process in Switzerland. *Waste Management*, 36, 33–43.

Caballero-Guzman A., Nowack B., 2016. A critical review of engineered nanomaterial release data: Are current data useful for material flow modeling? *Environmental Pollution*, 213, 502-517.

Chaúque E.F.C., Zvimba J.N., Ngila J.C., Musee N., 2014. Stability studies of commercial ZnO engineered nanoparticles in domestic wastewater. *Physics and Chemistry of the Earth*, 67–69, 140–144.

Chaúque E.F.C., Zvimba J.N., Ngila J.C., Musee N., 2016. Fate, behaviour, and implications of ZnO nanoparticles in a simulated wastewater treatment plant. *Water SA*, 42-1, 72-81.

Choi S., Johnston M.V., Wang G., Huang C.P., 2017. Looking for engineered nanoparticles (ENPs) in wastewater treatment systems: Qualification and quantification aspects. *Science of the Total Environment*, 590–591, 809–817.

Demirel B., 2016. The impacts of engineered nanomaterials (ENMs) on anaerobic digestion processes, *Process Biochemistry*, 51, 308-313.

Dulger M., Sakallioğlu T., Temizel I., Demirel B., Copty N.K., Onay T.T., Uyguner-Demirel C.S., Karanfil T., 2015. Leaching potential of nano-scale titanium oxide in fresh municipal solid waste. *Chemosphere*, 144, 1567-1572.

Dwivedi A.D., Ma L.Q.1, 2014. Biocatalytic Synthesis Pathways, Transformation, and Toxicity of Nanoparticles in the Environment. *Critical Reviews in Environmental Science and Technology*, 44, 1679–1739.

Dwivedi A.D., Dubey S.P., Sillanpää M., Kwon Y., Lee C., Varma R.S., 2015. Fate of engineered nanoparticles: Implications in the environment. *Environmental Pollution*, 287, 64–78.

Dolez, P.I., 2015. *Nanoengineering Global Approaches to Health and Safety Issues*, Elsevier, USA.

Garner K.L., Keller A.A., 2014. Emerging patterns for engineered nanomaterials in the environment: a review of fate and toxicity studies. *J Nanopart Res*, 16:2503, 1-28.

Goswami L., Kim K., Deep A., Das P., Bhattacharya S.S., Kumar S., Adelodun A.A., 2017. Engineered nano particles: Nature, behavior, and effect on the environment. *Journal of Environmental Management*, 196, 297-315.

Han Y., Kim D., Hwang G., Lee B., Eom I., Kim P.J., Tong M., Kim H., 2014. Aggregation and dissolution of ZnO nanoparticles synthesized by different methods: Influence of ionic strength and humic acid. *Colloids and Surfaces A: Physicochem. Eng. Aspects*, 451, 7–15.

Hou J., Miaoa L., Wanga C., Wang P., Ao Y., Qiana J., Dai S., 2014. Inhibitory effects of ZnO nanoparticles on aerobic wastewater biofilms from oxygen concentration profiles determined by microelectrodes. *Journal of Hazardous Materials*, 276, 164–170.

Hou J., Wu Y., Li X., Wei B., Li S., Wang X., 2018. Toxic effects of different types of zinc oxide nanoparticles on algae, plants, invertebrates, vertebrates and microorganisms. *Chemosphere*, 193, 852-860.

Jiang X., Tonga M., Lu R., Kim H., 2012. Transport and deposition of ZnO nanoparticles in saturated porous media. *Colloids and Surfaces A: Physicochemical and Engineering Aspects*, 401, 29– 37.

Joo S.H., Zhao D., 2017. Environmental dynamics of metal oxide nanoparticles in heterogeneous systems: A review. *Journal of Hazardous Materials*, 322, 29–47.

Keller A.A., McFerran S., Lazareva A., Suh S., 2013a. Global life cycle releases of engineered nanomaterials. *Journal of Nanoparticle Research*, 15, 1692.

Keller A.A., Lazareva A., 2013b. Predicted Releases of Engineered Nanomaterials: From Global to Regional to Local. *Environmental Science and Technology Letter* 2014, 1, 65–70.

Kiser M.A., Westerhoff P., Benn T., Wang Y., Perez-Rivera J., Hristovski K., 2009. Titanium nanomaterial removal and release from wastewater treatment plants. *Environmental Science and Technology*, 43, 6757-6763.

Kole C., Kumar D., Sakthi K., Mariya V., 2016. Plant Nanotechnology. In: Subbenaik S.C., (Eds), Chapter 2 Physical and Chemical Nature of Nanoparticles, Springer International Publishing.

Kwak, I.J., An, Y-J., 2016. The current state of the art in research on engineered nanomaterials and terrestrial environments: Different-scale approaches. *Environmental Research*, 151, 368-382.

Luther, W., 2004. Industrial application of nanomaterials- chances and risks, Technology analysis. Future Technologies Division of VDI Technologiezentrum GmbH, Düsseldorf Germany.

Ma H., Williams P.L., Diamond S.A., 2013. Ecotoxicity of manufactured ZnO nanoparticles- A review, *Environmental Pollution*, 172, 76-85.

Mueller N.C., Buha J., Wang J., Ulrich A., Nowack B., 2013. Modeling the flows of engineered nanomaterials during waste handling. *Environmental Sciences: Processes Impacts*, 15, 251.

Musee N., Nanowastes and the environment: Potential new waste management paradigm, *Environment International* 37 (2011) 112–128.

Nowack B., Ranville J.F., Diamond S., Gallegro-Urrea J., Metcalfe C., Rose J., Horne N., Koelmans A., Klaine S.J., 2012. Potential scenarios for nanomaterial release and subsequent alteration in the environment. *Environmental Toxicology Chemistry*, 31, 1, 50-59.

Omar F.M., Aziz H.A., Stoll S., 2014. Stability of ZnO Nanoparticles in Solution. Influence of pH, Dissolution, Aggregation and Disaggregation Effects. *Journal of Colloid Science and Biotechnology*, 3, 1–10.

Otero-Gonzalez L., Field J.A., Sierra-Alvarez R., 2014. Fate and long-term inhibitory impact of ZnO nanoparticles during high-rate anaerobic wastewater treatment. *Journal of Environmental Management*, 135, 110–117.

Pachapur, V.L., Larios, A.D., Cledón, M., Brar, S.K., Verma, M., Surampalli R.Y., 2016. Behavior and characterization of titanium dioxide and silver nanoparticles in soils. *Science of the Total Environment*, 563–564, 933–943.

Park C.M., Chu K.H., Heo J., Her N., Jang M., Son A., Yoon Y., 2016. Environmental behavior of engineered nanomaterials in porous media: a review. *Journal of Hazardous Materials*, 309, 133-150.

Part F., Berge N., Baran P., Stringfellow A., Sun W., Bartelt-Hunt S., Mitrano D., Li L., Hennebert P., Quicker P., Bolyard S.C, Huber-Humer M., 2018. A review of the fate of engineered nanomaterials in municipal solid waste streams. *Waste Management*, 75, 427–449.

Peng Y.H., Tso C.P., Tsai Y.C, Zhuang C.M., Shih Y.H., 2015. The effect of electrolytes on the aggregation kinetics of three different ZnO nanoparticles in water. *Science of the Total Environment*, 530–531, 183–190.

Puay N., Qiu G., Ting Y., 2015. Effect of Zinc oxide nanoparticles on biological wastewater treatment in a sequencing batch reactor. *Journal of Cleaner Production*, 88, 139-145.

Ramakrishnan A., Blaney L., Kao J., Tyagi R.D., Zhang T.C., Surampalli R.Y., 2015. Emerging contaminants in landfill leachate and their sustainable management. *Environmental Earth Science*, 73, 1357-1368.

Reinhart D., Berge N., Santra S., Bolyard S.C., 2010. Emerging contaminants: Nanomaterial fate in landfills. *Waste Management*, 30, 202-2021.

Rodrigues, S.M., Trindade, T., Duarte, A.C., Pereira, E., Koopmans, G.F., Romkens, P.F.A.M., 2016. A framework to measure the availability of engineered nanoparticles in soils: Trends in soil tests and analytical tools. *Trends in Analytical Chemistry*, 75, 129–140.

Sakallioğlu T., Bakirdoven M., Temizel I., Demirel B., Coptý N.K., Onay T.T., Uyguner Demirel C.S., Karanfil T., 2016. Leaching of nano-ZnO in municipal solid waste. *Journal of Hazardous Materials*, 317, 319–326.

Sabir S., Arshad M., Chaudhari S.K., 2014. Zinc Oxide Nanoparticles for Revolutionizing Agriculture: Synthesis and Applications. *Scientific World Journal*, 2014, 0-8.

Salieri B., Turner D.A., Nowack B., Hirschier R., 2018. Life cycle assessment of manufactured nanomaterials: Where are we? *NanoImpact*, 10, 108–120.

Singh, A.K., 2016. *Engineered Nanoparticles Structures, Properties and Mechanism of Toxicity*, Elsevier, U.S.A.

Sirelkhatim A., Mahmud S., Seeni A., Kaus N.H.M., Ann L.C., Bakhori S.K.M., Hasan H., Mohamad D., 2015. Review on Zinc Oxide Nanoparticles: Antibacterial Activity and Toxicity Mechanism. *Nano-Micro Lett.*, 7(3), 219–242.

Sturikova H., Krystofova O., Huska D., Adam V., 2018. Zinc, zinc nanoparticles and plants. *Journal of Hazardous Materials* 349, 101–110.

Sweet L., Strohm B., 2006. Nanotechnology-life cycle risk management. *Human Ecological Risk Assessment*, 12, 528-551.

Tan M., Qiu G., Ting Y. 2015. Effects of ZnO nanoparticles on wastewater treatment and their removal behavior in a membrane bioreactor. *Bioresource Technology*, 185, 125–133.

Temizel I., Emadian S. M., Di Addario M., Onay T.T., Demirel B., Coptý N.K., Karanfil T., 2017. Effect of nano-ZnO on biogas generation from simulated landfills. *Waste Management*, 63, 18–26.

Theodore L., Kunz R.G., 2005. *Nanotechnology: Environmental Implications and Solution*. In: Shelley S.A. (Eds), Chapter 2 Nanotechnology: Turning Basic Science Into Reality.

TSE EN ISO 11885, 2013. Water quality- Determination of selected by inductively coupled plasma optical emission spectrometry (ICP-OES) Turkish Standards Institution, Ankara, Turkey.

Wanga J., Chen R., Xiang L., Komarnenic S., 2018. Synthesis, properties and applications of ZnO nanomaterials with oxygen vacancies: A review. *Ceramics International*, 44, 7357-7377.

Wang D., Lin Z., Wang T., Yao Z., Qin M., Zheng S., Lu W., 2016. Where does the toxicity of metal oxide nanoparticles come from: The nanoparticles, the ions, or a combination of both?. *Journal of Hazardous Materials*, 308, 328–334.

Weinberg H., Galyean A., Leopold M., 2011. Evaluating engineered nanoparticles in natural waters, *Trends in Analytical Chemistry*, 30-1, 72-83.

Weir A., 2011. TiO₂ nanomaterials: Human exposure and environmental release. M.Sc. Thesis, Arizona State University, U.S.A.

Wu Q., Huang K., Sun H., Ren H., Zhang X., Ye L., 2018. Comparison of the impacts of zinc ions and zinc nanoparticles on nitrifying microbial community. *Journal of Hazardous Materials*, 343,166–175.

Xiao-hong Z., Bao-cheng H., Tao Z., Yan-chen L., Han-chang S., 2015. Aggregation behavior of engineered nanoparticles and their impact on activated sludge in wastewater treatment. *Chemosphere*, 119, 568–576.

Xu Y., Wang C., Hou J., Dai S., Wang P., Miao L., Lv B., Yang Y., You G., 2016. Effects of ZnO nanoparticles and Zn²⁺ on fluvial biofilms and the related toxicity mechanisms. *Science of the Total Environment*, 544, 230-237.

Yang Y., Zhang C., Hu Z., 2013. Impact of metallic and metal oxide nanoparticles on wastewater treatment and anaerobic digestion. *Environmental Science: Process & Impacts*, 15, 39-48.

Yechezkel Y., Ishai D., Brian B., 2016. Transport of engineered nanoparticles in partially saturated sand columns. *Journal of Hazardous Materials*, 311, 254–262.

Zhang X., Zhang N., Fu H., Chen T., Liu S., Zheng S., Zhang J., 2017. Effect of zinc oxide nanoparticles on nitrogen removal, microbial activity and microbial community of CANON process in a membrane bioreactor. *Bioresource Technology*, 243, 93–99.

APPENDIX: THE COMPLETE RESULTS FROM SET 1 TO SET 9

Table 1. The pH recordings of uncoated ZnO NP acidic set reactors with time (Set 1).

Time	0 mg/L	10 mg/L	25 mg/L	100 mg/L
0	5.25	5.1	4.99	5.13
1	5.21	5.09	4.9	5.23
2	5.09	5.03	5.11	5.01
3	4.89	4.92	6.23	5.86
4	5.9	4.91	6.03	5.5
5	4.83	4.86	5.81	4.95
6	5.22	5.27	5.92	5
12	5.49	5.7	6.13	5.64
24	5.27	5.31	5.99	5.95
36	5.38	6.25	6.14	6.35
48	5.14	5.67	5.6	5.62
60	6.01	6.41	6.17	6.16
72	6.02	6.15	6.05	5.94

Table 2. The Zn concentrations values of uncoated ZnO NP acidic set reactors with time (Set 1).

Time	0 mg/L	10 mg/L	25 mg/L	100 mg/L
0	5.31	7.44	18.6	46.86
1	4.18	6.96	17.4	42.32
2	5.76	6.53	16.33	40.85
3	4.62	6.01	15.03	35.83
4	5.02	6.31	15.78	37.55
5	4.5	5.85	14.63	38.61
6	4.84	5.54	13.85	37.08
12	4.61	6.39	15.98	31.12
24	4.68	4.42	11.05	24.07
36	5.95	2.84	7.1	14.61
48	4.87	3.07	7.675	14.81
60	4.89	2.83	7.075	12.66
72	4.39	2.22	5.55	18.46

Table 3. The pH recordings of uncoated ZnO NP basic set reactors with time (Set 2).

Time	0 mg/L	10 mg/L	25 mg/L	100 mg/L
0	11.24	12.25	12.19	12.06
1	10.51	10.25	11.69	10.9
2	9.25	10	11.65	11.65
3	9.81	9.88	11.15	10.29
4	8.56	10.03	10.93	11.18
5	7.56	6.99	10.87	9.12
6	9.5	7.2	10.35	10
12	6.97	6.16	7.01	7.82
24	6.81	6.34	6.78	6.64
36	6.71	6.64	6.38	6.85
48	6.25	6.17	6.27	6.33
60	6.83	6.61	6.64	6.74
72	6.46	6.62	6.36	6.49

Table 4. The Zn concentrations values of uncoated ZnO NP basic set reactors with time (Set 2).

Time	0 mg/L	10 mg/L	25 mg/L	100 mg/L
0	3.59	6.32	17.25	44.81
1	4.1	6.64	18.24	39.58
2	4.48	5.92	16.7	36.68
3	3.47	4.7	7.14	30.11
4	4.21	4.96	9.15	29.96
5	2.57	2.82	7.27	28.96
6	5.01	3.41	7.54	27.96
12	2.96	2.37	3.2	19.2
24	3.6	2.93	3.07	20.09
36	2.35	1.7	2.57	17.3
48	3.14	1.83	3.48	15.15
60	2.57	1.48	2.27	8.56
72	1.98	1.05	2.56	7.08

Table 5. The pH recordings of uncoated ZnO NP high IS set reactors with time (Set 3).

Time	0 mg/L	10 mg/L	25 mg/L	100 mg/L
0	6.07	5.03	5.35	5.73
1	5.81	5.13	5	5
2	5.65	5.24	4.39	4.64
3	5.66	5.01	4.91	5.21
4	5.53	4.69	4.3	5.91
5	5.72	5	5.61	5.34
6	5.7	5.3	5.14	5
12	6.46	5.27	4.8	5.63
24	6.54	5.35	4.88	5.81
36	5.03	5.57	6.72	6.39
48	4.51	5.34	6.39	5.7
60	5.04	6.22	6.75	6.19
72	4.89	6.14	6.61	6.07

Table 6. The Zn concentrations values of uncoated ZnO NP high IS set reactors with time (Set 3).

Time	0 mg/L	10 mg/L	25 mg/L	100 mg/L
0	0.42	5.16	16.37	47.27
1	2.37	5.78	17.46	19.36
2	2.1	6.81	15.86	17.31
3	3.36	3.91	16.59	16.51
4	2.08	5.73	20.2	16.7
5	2.38	6.32	18.81	18.61
6	1.49	5.91	19.8	17.73
12	1.13	5.46	16.33	14.18
24	0.99	6.11	8.27	12.58
36	6.5	5.46	2.75	11.46
48	3.92	5.72	3.54	10.69
60	5.99	3.85	2.26	8.16
72	5.54	3.63	1.75	7.9

Table 7. The conductivity recordings of uncoated ZnO NP high IS set reactors with time (Set 3).

Time	0 mg/L	10 mg/L	25 mg/L	100 mg/L
0	6.07	5.03	5.35	5.73
1	5.81	5.13	5	5
2	5.65	5.24	4.39	4.64
3	5.66	5.01	4.91	5.21
4	5.53	4.69	4.3	5.91
5	5.72	5	5.61	5.34
6	5.7	5.3	5.14	5
12	6.46	5.27	4.8	5.63
24	6.54	5.35	4.88	5.81
36	5.03	5.57	6.72	6.39
48	4.51	5.34	6.39	5.7
60	5.04	6.22	6.75	6.19
72	4.89	6.14	6.61	6.07

Table 8. The pH recordings of coated ZnO NP acidic set reactors with time (Set 4).

Time	0 mg/L	10 mg/L	25 mg/L	100 mg/L
0	5.2	5	4.72	5.65
1	5.83	5.78	5.62	5.25
2	5.77	5.84	5.68	5.77
3	5.9	5.96	5.79	5.95
4	5.71	6.19	5.95	5.96
5	5.78	5.98	6	6.13
6	5.82	5.96	5.85	6.01
12	5.76	6.03	5.81	5.91
24	5.78	5.92	5.61	5.88
36	5.81	5.79	5.69	5.87
48	5.85	5.57	5.68	5.88
60	5.94	5.8	5.87	6.14
72	5.3	5.07	5.13	5.4

Table 9. The Zn concentrations values of coated ZnO NP acidic set reactors with time (Set 4).

Time	0 mg/L	10 mg/L	25 mg/L	100 mg/L
0	4.03	2.72	3.01	13.45
1	3.9	1.63	2.78	15.22
2	1.98	2.17	2.53	10.34
3	2.99	1.97	2.61	8.78
4	3.22	1.77	2.34	9.89
5	4.01	1.89	3.17	9.2
6	2.91	1.19	2.51	8.27
12	1.3	0.8	2.23	5.5
24	2.3	1.32	2.09	8.58
36	1.29	1.02	1.95	6.81
48	1.22	0.92	1.79	5.04
60	1.02	1.43	2.51	8.11
72	2.41	1.95	2.42	3.49

Table 10. The pH recordings of coated ZnO NP basic set reactors with time (Set 5).

Time	0 mg/L	10 mg/L	25 mg/L	100 mg/L
0	11.77	11.8	11.66	11.66
1	11.95	11.96	11.73	11.84
2	11.66	11.7	11.59	11.58
3	11.65	11.67	11.22	11.54
4	11.56	11.66	11.31	11.6
5	11.71	11.65	11.45	11.59
6	11.69	11.65	11.09	11.54
12	11.53	11.52	11.08	11.39
24	9.98	11.48	9.82	10.86
36	8.55	10	8.75	9.1
48	7.6	8.94	7.52	7.46
60	7.4	8.6	7.6	7.14
72	6.6	7.8	8.28	6.16

Table 11. The Zn concentrations values of coated ZnO NP basic set reactors with time (Set 5).

Time	0 mg/L	10 mg/L	25 mg/L	100 mg/L
0	1.9	9.18	7.53	30
1	3.66	4.44	9.37	25.53
2	1.86	3.64	5.96	24.27
3	2.1	7.36	4.85	23
4	1.61	3.7	7	21.26
5	3.62	8.64	8.74	15.92
6	2.19	8.76	5.67	15.58
12	2.06	3.7	3.85	15.24
24	3.22	4.94	4.65	12.81
36	2.6	2.63	5.44	9.86
48	2.17	4.88	5.25	8.74
60	2.14	5.4	3.65	6.07
72	1.99	6.58	2.61	11.05

Table 12. The pH recordings of coated ZnO NP high IS set reactors with time (Set 6).

Time	0 mg/L	10 mg/L	25 mg/L	100 mg/L
0	7.09	7.28	7.68	7.21
1	7.1	7.39	7.53	7.18
2	6.65	6.82	6.69	6.53
3	6.83	6.69	6.79	6.46
4	6.43	6.6	6.74	6.34
5	6.59	6.52	6.62	6.24
6	6	6.42	6.63	6.27
12	5.45	6.2	6.37	5.99
24	5.89	5.86	6.06	5.73
36	4.96	5.87	6.06	5.41
48	4.39	5.76	5.81	5.2
60	4.64	5.91	6.04	5.45
72	5.73	5.46	5.73	5.11

Table 13. The Zn concentrations values of coated ZnO NP basic set reactors with time (Set 6).

Time	0 mg/L	10 mg/L	25 mg/L	100 mg/L
0	0.72	1	7.02	15.88
1	1.43	2.68	6.94	18.09
2	1.14	1.6	8.01	15.5
3	0.99	1.7	7.05	12.91
4	2.03	1.43	6.29	10.97
5	1.67	1.64	7.1	10.94
6	1.3	1.06	7.36	12.13
12	1.11	1.13	4.52	13.31
24	0.79	1.31	3.98	12.66
36	1	1.5	2.1	7.6
48	1.04	1.38	3.67	7.71
60	1.12	1.32	1.5	8.98
72	0.82	0.84	4.73	9.14

Table 14. The conductivity recordings of coated ZnO NP high IS set reactors with time (Set 6).

Time	0 mg/L	10 mg/L	25 mg/L	100 mg/L
0	5.34	3.77	5.37	4.62
1	5.38	4.69	6.37	5.74
2	6.5	5.42	6.69	6.13
3	6.37	5.69	7.22	6.15
4	6.69	6.03	7.09	6.2
5	6.99	6.12	7.84	6.17
6	7.03	6.17	8.84	7.95
12	8.3	7.02	8.94	8.25
24	8.36	7.68	9.07	9.1
36	10.32	8.18	9.9	9.68
48	10.3	8.47	10.07	9.87
60	9.63	8.6	10.26	10.18
72	9.93	8.26	10.53	12

Table 15. The pH recordings of dispersion ZnO NP acidic set reactors with time (Set 7).

Time	0 mg/L	10 mg/L	25 mg/L	100 mg/L
0	6.5	4.5	6	6.3
1	6.6	6.3	6.8	7.1
2	6.9	6.8	6.9	7.4
3	6.7	5.9	6.2	6.6
4	6.8	6.2	6.2	6.7
5	6.8	6.4	6.2	6.7
6	6.7	6.4	6.1	6.7
12	6.4	6	5.6	6.5
24	5.3	5.3	4.9	5.8
36	5.5	5.2	4.9	6
48	5.8	5.6	5.3	6.3
60	6	5.8	5.3	6
72	5.9	5.7	5.6	5.9

Table 16. The Zn concentrations values of dispersion ZnO NP acidic set reactors with time (Set 7).

Time	0 mg/L	10 mg/L	25 mg/L	100 mg/L
0	0.93	4.01	13.09	32.54
1	2.96	3.16	15.51	37.21
2	4.9	2.75	10.99	28.58
3	2.7	2.04	6.93	24.55
4	2.2	2.41	6.48	21.29
5	2.01	2.35	6.23	20.32
6	2.2	2.35	5.67	22.81
12	2.29	2	6.74	21.07
24	2.25	2.71	8.17	19.38
36	5.07	2.89	9.6	19.44
48	7.12	2.55	10.22	17.88
60	2.74	2.77	6.5	18.41
72	1.78	1.91	5.01	16.55

Table 17. The pH recordings of dispersion ZnO NP basic set reactors with time (Set 8).

Time	0 mg/L	10 mg/L	25 mg/L	100 mg/L
0	12.7	12.7	13.2	13.1
1	12.8	12.9	13	13
2	12.9	12.8	12.8	12.9
3	12.4	12.6	12.6	12.4
4	12.4	12.6	12.5	12.5
5	12.2	12.5	12.5	12.5
6	12.2	12.5	12.5	12.4
12	12	12.4	12.4	12.4
24	10.5	10.1	12.1	12.1
36	8.9	9	11.2	11.8
48	5.3	7.5	9.4	10.4
60	5.5	7.2	6.9	8.8
72	5.5	7.1	7	6.6

Table 18. The Zn concentrations values of dispersion ZnO NP basic set reactors with time (Set 8).

Time	0 mg/L	10 mg/L	25 mg/L	100 mg/L
0	0.52	5.71	14.19	44.35
1	1.15	5.17	12.12	44.31
2	0.85	4.26	11.01	45.01
3	0.93	ND	9.57	44.34
4	1.24	ND	8.45	42.62
5	0.76	ND	8.33	39.05
6	1.5	ND	7.81	42.06
12	0.83	ND	7.02	37.53
24	1.61	13.37	6.43	35.53
36	2.56	13.18	5.01	34.01
48	1.09	4.8	6.22	30.92
60	1.59	2.94	6.61	24.76
72	0.75	2.54	5.11	19.55

*ND: Non-detected.

Table 19. The pH recordings of dispersion ZnO NP high IS set reactors with time (Set 9).

Time	0 mg/L	10 mg/L	25 mg/L	100 mg/L
0	7.1	7.3	7.5	7.1
1	7.5	7.5	7.8	7.2
2	7.7	7.4	7.7	7.2
3	6.9	6.9	7.3	6.6
4	7.1	7.1	7.3	6.7
5	7	7.1	7.3	6.6
6	7	7	7.3	6.6
12	6.7	6.8	7	6.4
24	5.4	6.3	6.6	5.2
36	5.2	6.2	6.5	4.9
48	5.1	6.1	6.3	4.5
60	5.1	6	6.4	4.5
72	5.1	5.9	6.2	4.2

Table 20. The Zn concentrations values of dispersion ZnO NP high IS set reactors with time (Set 9).

Time	0 mg/L	10 mg/L	25 mg/L	100 mg/L
0	0.46	4.61	16.77	51.6
1	0.61	2.96	9.8	39.1
2	0.95	2.5	6.64	32.4
3	0.98	1.6	5.58	23.99
4	0.63	1.86	4.99	20.96
5	1.09	1.47	4.9	17.51
6	0.54	1.57	4.81	18.77
12	0.58	10.1	6.78	21.72
24	0.73	2.37	10.22	17.69
36	1.2	1.47	8.57	17.19
48	0.9	1.6	11.59	21.33
60	1.1	1.82	11.72	25.2
72	1.74	2.18	10	22.73

Table 21. The conductivity recordings of coated ZnO NP high IS set reactors with time (Set 9).

Time	0 mg/L	10 mg/L	25 mg/L	100 mg/L
0	3.18	3.81	3.99	4.52
1	3.7	4.01	4.06	4.3
2	4.06	4.32	4.31	4.35
3	4.17	4.57	4.43	4.44
4	4.24	4.65	4.52	4.44
5	4.37	4.74	4.56	4.55
6	4.46	4.77	4.63	4.61
12	4.56	4.88	4.69	4.64
24	4.95	5.29	4.93	5.13
36	5.09	5.43	4.94	5.37
48	4.96	5.23	4.8	5.03
60	5.12	5.49	4.99	5.51
72	4.72	5.26	4.53	5.03